# Mechanistic Investigation of the Ru-Catalyzed Hydroamidation of Terminal Alkynes

Matthias Arndt, Kifah S. M. Salih, Andreas Fromm, Lukas J. Goossen,* Fabian Menges, and Gereon Niedner-Schatteburg*

Fachbereich Chemie and State Reasearch Center OPTIMAS, TU Kaiserslautern, Erwin-Schrödinger-Strasse 52–54, 67663 Kaiserslautern, Germany

S *Supporting Information*

ABSTRACT: The ruthenium-catalyzed hydroamidation of terminal alkynes has evolved to become a broadly applicable tool for the synthesis of enamides and enimides. Depending on the catalyst system employed, the reaction leads chemo-, regio-, and stereoselectively to a single diastereoisomer. Herein, we present a comprehensive mechanistic study of the ruthenium-catalyzed hydroamidation of terminal alkynes, which includes deuterium-labeling, in situ IR, in situ NMR, and in situ ESI—MS experiments complemented by computational studies. The results support the involvement of ruthenium—hydride and ruthenium—vinylidene species as the key intermediates. They are best explained by a reaction pathway that consists of an oxidative addition of the amide, followed by insertion of a π-coordinated alkyne into a ruthenium—hydride bond, rearrangement to a vinylidene species, nucleophilic attack of the amide, and finally reductive elimination of the product.
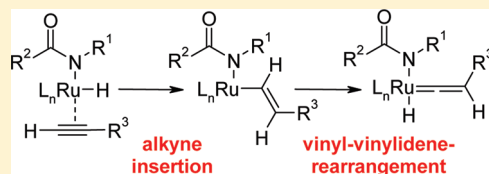
INTRODUCTION

Enamides are valuable structural elements in natural products with interesting biological activities and in pharmaceutical drug lead compounds[1] showing antibiotic,[2] antitumor,[3] anthelmintic,[4] antifungal, and cytotoxic activities (Figure 1).[5]

In addition, enamides can serve as versatile synthetic intermediates, particularly in pericyclic and photochemical reactions for the formation of heterocycles,[6] [4 + 2]-cycloadditions,[7] cross-coupling reactions,[8] Heck olefinations,[9] enantioselective additions,[10] or asymmetric hydrogenations.[11]

Traditional syntheses include the condensation of aldehydes and ketones with amides or dehydration of hemiaminals,[12] the Curtius rearrangement of α,β-unsaturated acyl azides,[13] and the elimination of β-hydroxy-α-silylamides (Peterson reaction).[14] Several metal-catalyzed approaches have also been investigated, such as the isomerization of N-allylamides[15] and catalytic cross-coupling reactions of amides and vinyl halides, pseudohalides or enol ethers.[16] Problems often encountered using these methods are the harsh reaction conditions, the formation of (E)- and (Z)-product mixtures, or the use of expensive or poorly available starting materials.

Over the last years, a particularly convenient synthetic entry to this important substrate class has emerged, namely, the addition of amides to terminal alkynes (Scheme 1).

This reaction mode is the most atom-economic transformation of all the catalytic reactions based on carboxylic acid derivatives that we have investigated over the last years.[17] On the basis of pioneering studies by Heider et al.[18] and Watanabe et al.,[19] who were the first to observe that ruthenium complexes mediate the addition of certain amides to terminal alkynes, we have developed

efficient Ru catalysts and established the addition of amide-type nucleophiles to terminal alkynes as a general method for the synthesis of enamide derivatives. The same reaction principle is the basis for a number of preparatively useful Ru-catalyzed addition reactions to alkynes, for example, their hydration with formation of aldehydes,[20] the addition of carboxylic acids to give enol esters,[21] their hydroamination with formation of imines or enamines,[22] their hydrothiolation to vinyl sulfides,[23] and the addition of alcohols to form vinyl ethers.[24]

Over the last years, a range of customized protocols were disclosed for the *anti*-Markovnikov addition of various N-nucleophilic amides, thioamides, and imides across terminal C—C triple bonds. They provide an expedient and chemo-, regio-, and stereoselective synthetic entry to enamides, thioenamides, and enimides (Scheme 2).

With a catalyst system generated in situ from bis(2-methallyl)-(cycloocta-1,5-diene)ruthenium(II) [(cod)Ru(met)$_2$], tri-n-butylphosphine (P(n-Bu)$_3$), and 4-dimethylaminopyridine (DMAP), tertiary (E)-enamides can be synthesized in high yields and selectivities from terminal alkynes and secondary amides.[25] The stereoselectivity can be reversed in favor of the corresponding (Z)-enamides when employing bis-(dicyclohexylphosphino)methane (dcypm) and water instead of P(n-Bu)$_3$ and DMAP. The reaction proceeds smoothly even in the presence of sensitive functional groups such as esters, ethers, ketones, halides, or silanes. Various amides, anilides, ureas, bislactams, carbamates, and even amide-type chiral auxiliaries can be
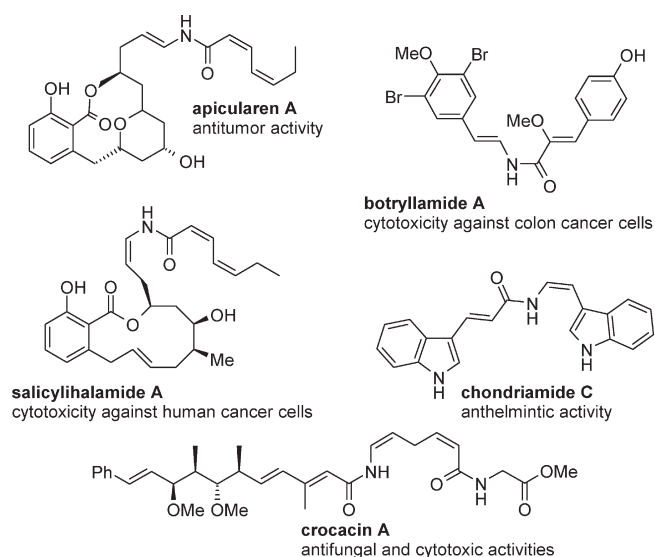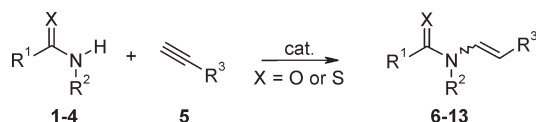
Figure 1. Enamide substructure in bioactive or functional molecules.

Scheme 1. Addition of Amides to Terminal Alkynes

used as N—H nucleophiles. Recently, we have shown that for many substrates, a similar level of activity can be achieved when the catalytically active species is generated in situ from inexpensive ruthenium trichloride hydrate $(RuCl_3 \cdot 3H_2O)$, $P(n\text{-}Bu)_3$, DMAP, K_2CO_3, and water.[26]

Subsequently, modified catalyst systems were developed that allowed extending the substrate scope to thioamides[27] and imides.[28] In this context, we made the discovery that for imides, which are acidic N—H nucleophiles, the addition of a Lewis acid rather than an auxiliary base is essential for achieving turnover of the catalyst.

The conversion of primary amides into secondary enamides is challenging due to the higher nucleophilicity of secondary over primary amides, leading to double vinylation products. However, a catalyst system consisting of the Lewis acid ytterbium(III) triflate in combination with $(cod)Ru(met)_2$ and an electron-rich, sterically demanding bidentate ligand (dcypb, 1,4-bis(dicyclohexylphosphino)butane) allowed the selective conversion of primary amides to secondary enamides.[29] This protocol gives access to (Z)-enamides in high yields and selectivities, whereas the (E)-enamides can be prepared by subsequent in situ double-bond isomerization with triethylamine at higher reaction temperatures in the same pot. Furthermore, after minor modifications, the same bimetallic system can be used for the Z-selective addition of secondary amides and imides to terminal alkynes in the absence of the primary amide functionality, yielding the corresponding enamides and enimides with Z/E-selectivities greater than 20:1.[30]

The applicability of Ru-catalyzed hydroamidation reactions is illustrated in Figure 2. The examples include the natural products alatamide, lansiumamides A and B, lansamide I, and botryllamides C and E.[29,31] They demonstrate that the hydroamidation of alkynes has meanwhile reached a high level of maturity and can

be widely applied in organic synthesis. However, the reaction mechanism has so far remained speculative.

The aims of the present study were to investigate the coordination type of the alkyne during the reaction, to clarify how the regio- and stereochemistry is controlled, and to identify the rate-determining step of the catalytic cycle.

■ MECHANISTIC CONSIDERATIONS

Numerous potential reaction mechanisms have to be evaluated with appropriately designed mechanistic studies and control experiments.

Several catalytic cycles have previously been proposed for the Ru-catalyzed addition of nucleophiles such as amides, amines, carboxylic acids, and water to C—C triple bonds. The first mechanism for *anti*-Markovnikov-selective hydroamidations was postulated by Watanabe but was not supported by experimental data (Scheme 3).[19]

This mechanism will further be referred to as *Mechanism A*. It involves the oxidative addition of an amide, insertion of a π-coordinated alkyne into the Ru—N or Ru—H bond, and reductive elimination of the enamide product. Stabilizing interactions between the oxygen atom of the carbonyl group and the Ru center in a four- or six-membered intermediate (**17** and **18**) that forms following alkyne insertion were used to explain the regioselectivity, in both cases leading to the formation of the *anti*-Markovnikov product. Uchimaru proposed a similar mechanism for the Markovnikov-selective Ru-catalyzed hydroamination of terminal alkynes,[22a] in which a π-coordinated alkyne inserts into the Ru—N bond of a Ru-amine species. The Markovnikov selectivity is explained by the formation of a sterically less hindered Ru-enamine intermediate.

Indications for *Mechanism A* would be provided by a dependence of the rate-determining step on the acidity of the amide and the electronic and steric properties of the Ru-complex. Moreover, Ru-hydride species may be detectable via ^1H NMR or electronspray ionization mass spectroscopy (ESI—MS) investigations if concentrations are high enough, and the reaction of 1-deuterioalkynes should give rise to a product deuterated exclusively in the 1-position.

Dixneuf proposed a different mechanism to explain the selective formation of *anti*-Markovnikov addition products in the addition of carboxylic acids to alkynes. His pathway can directly be translated to hydroamidation reactions (Scheme 4).[32]

This mechanism will further be referred to as *Mechanism B*. Its key step is the formation of a Ru—vinylidene complex **20** via a 1,2-proton shift at the alkyne moiety, followed by an attack of a nucleophile in the α-position to the ruthenium center. After protonolysis of the ruthenium intermediate **25** and regeneration of the active ruthenium species **19**, an *anti*-Markovnikov enol ester **26** or enamide **6—13** is formed. In contrast, the alternative direct addition of a nucleophile to a coordinated alkyne should result in the formation of the Markovnikov product. This mechanism provides a sound explanation for the *anti*-Markovnikov selectivity of the reaction and its limitation to terminal alkynes. Experiments with isolated Ru—vinylidene complexes confirmed that their reaction with nucleophiles will indeed lead to the addition product. As an alternative to vinylidene formation via a 1,2-proton shift, a sequence consisting of an oxidative addition of the alkyne C(sp)—H bond to ruthenium followed by a 1,3-proton shift was also proposed as an entry to this mechanism.

Mechanism B would again predict a dependence of the reaction rate on the electronic and steric properties of the Ru-complex,
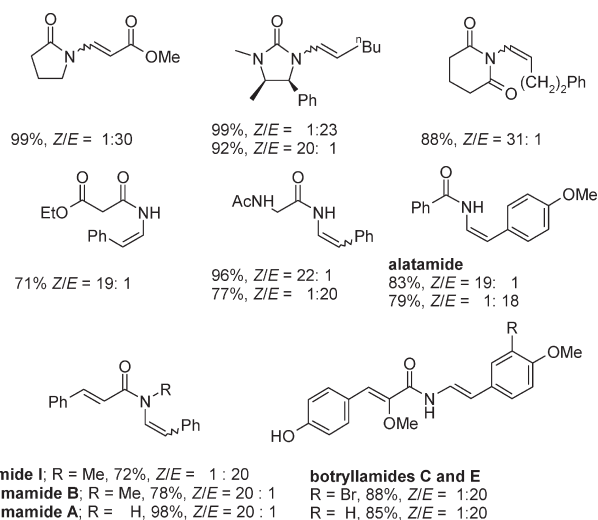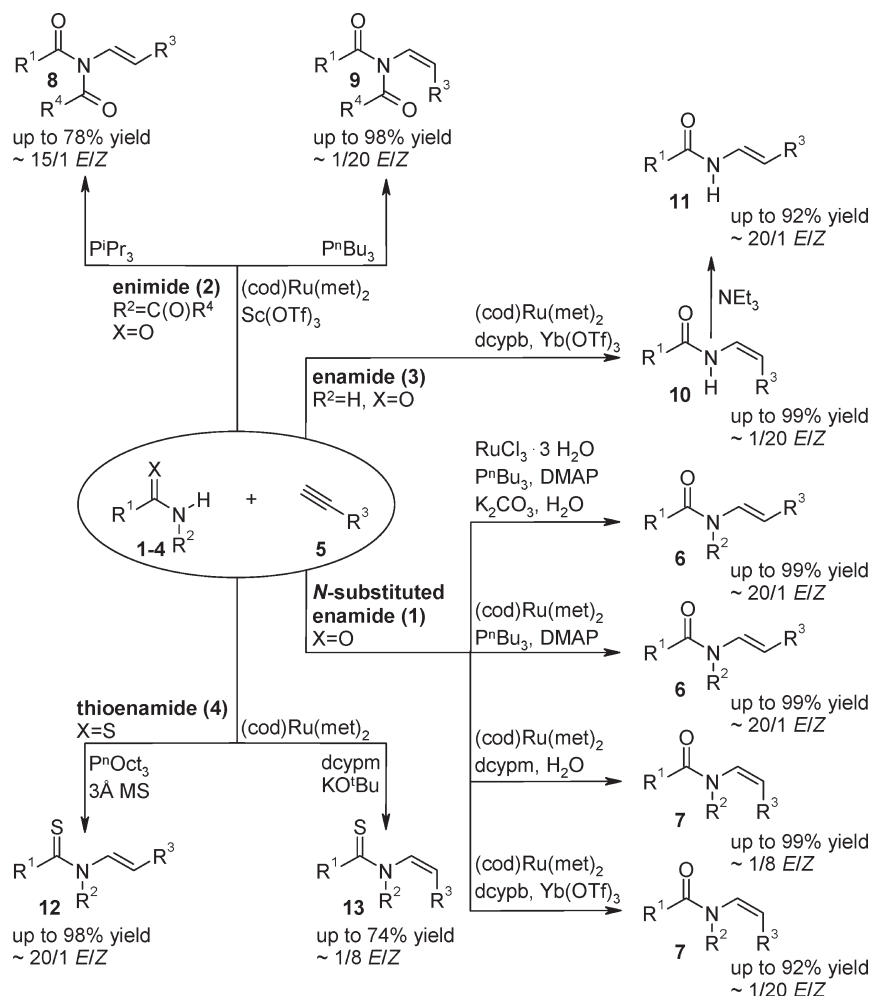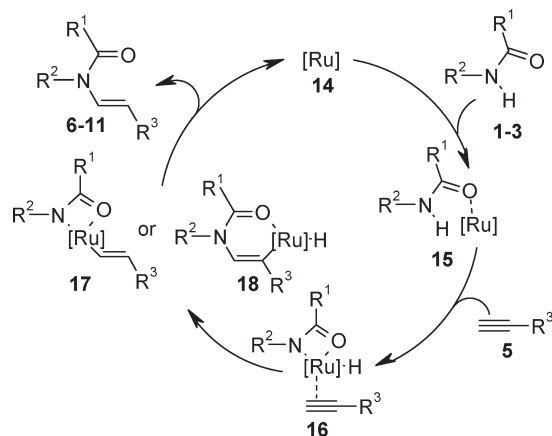
Scheme 2. Ru-catalyzed Addition of *N*-Nucleophiles to Terminal Alkynes

Figure 2. Representative example for the addition of terminal alkynes.

Scheme 3. *Mechanism A*: Hydroamidation Pathway Postulated by Watanabe


and the reaction would benefit from the stabilizing effect of electron-donating ligands on the high oxidation state of the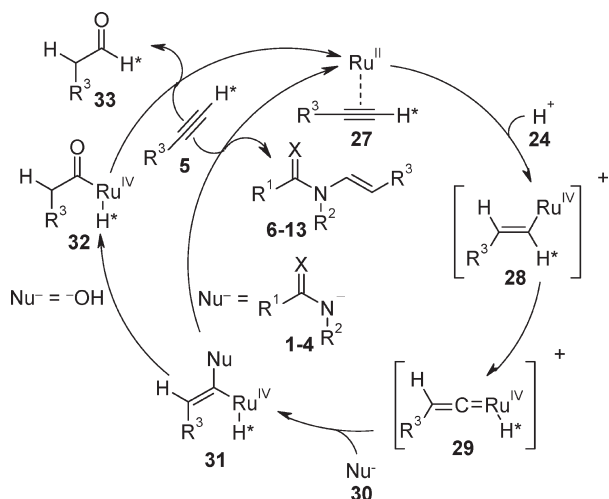 ruthenium center. We assume the vinylidene formation to be a relatively slow reaction step. Therefore, in contrast to *Mechanism A*, the acidity of the alkyne C(sp)−H bond rather than that of the amide N−H bond should have an additional influence on the C−H bond cleaving vinylidene formation step. Therefore,

Scheme 4. *Mechanism B:* Hydroamidation in Analogy to Dixneuf's Carboxylation of Terminal Alkynes
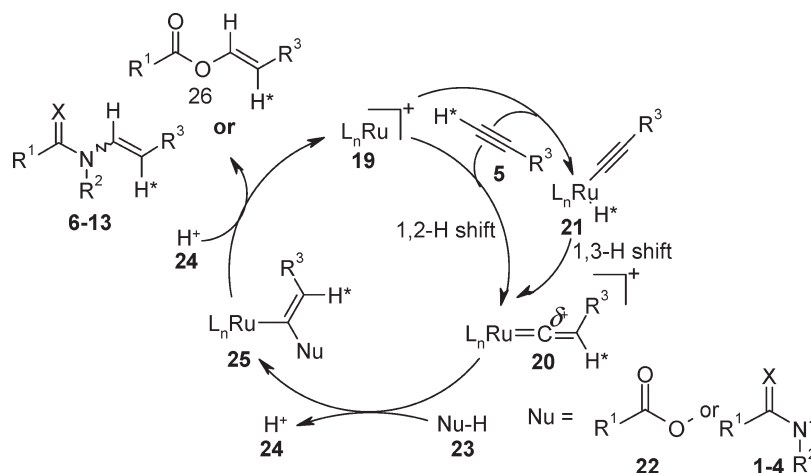
Scheme 5. *Mechanism C:* Hydroamidation in Analogy to Wakatsuki's Hydration of Terminal Alkynes

Scheme 6. *Mechanism D:* Hydroamidation via Oxidative Addition of the Amide, Insertion of the Alkyne, and Ru—Vinyl/—Vinylidene Rearrangement
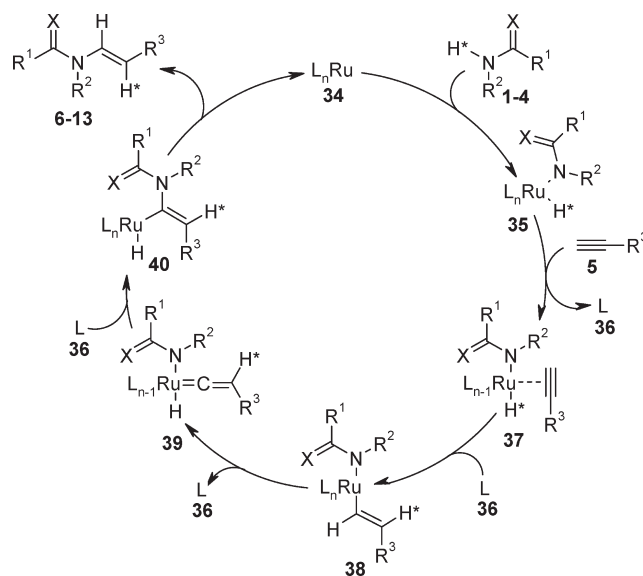

kinetic isotope effects should be measurable in experiments with 1-deuterioalkynes, and the resulting product should exclusively be deuterated in the 2-position, because proton shifts to the internal alkyne C-atom are postulated. ESI—MS and in situ IR experiments could help to verify reactive intermediates.

Vinylidene intermediates have been confirmed for other ruthenium-catalyzed addition reactions.[32] One example is the addition of alcohols to alkynes, where a 1,2-proton shift was observed in isotopic labeling experiments.[24b] However, the intermediacy of vinylidene intermediates does not necessarily call for proton shifts, and alternative mechanisms for Ru—vinylidene formation have been proposed for the hydration of terminal alkynes[20b] and for stoichiometric reactions of terminal alkynes with ruthenium—hydride complexes.[33] On the basis of computational studies, Wakatsuki and Caulton concluded that vinylidene intermediates are formed via rearrangement of Ru-vinyl species for these reactions, whereas pathways via 1,2- or 1,3-proton shifts are energetically unfavorable (see Schemes 5 and 6).

For the hydration of terminal alkynes, the absence of proton shifts was corroborated by deuterium-labeling experiments.

Wakatsuki et al. thus derived a different mechanism involving Ru—vinylidene intermediates.[20b] Again, this may be translated to hydroamidation reactions (Scheme 5).

The key step in this mechanism, which will further be referred to as *Mechanism C*, is the protonation of a π-coordinated alkyne resulting in the formation of a cationic Ru^{IV}—vinyl intermediate **28**. Its rearrangement to the Ru—H—vinylidene species **29** was proposed to be the rate-determining step. Addition of a nucleophile and reductive elimination gives the aldehyde **33** or the enamide **6−13**, respectively. In this mechanism, the alkyne C(sp)-proton is transferred to the metal center and subsequently reattached to its original carbon atom. For the hydration of alkynes, 1,2-proton shifts were indeed not observed in deuteration studies. This mechanism offers an explanation for the *anti*-Markovnikov selectivity and the limitation to terminal alkynes. However, it involves cationic intermediates in the high oxidation states of +4 or even +6, depending on whether the Ru=C bond in species **29** is

viewed as a covalent bond or a as the coordination of a neutral carbene ligand to the metal center. This may be reasonable for hydration reactions in aqueous solvents, but is less likely for hydroamidations under almost neutral conditions in toluene.

If the hydroamidation proceeded via *Mechanism C*, the use of protic and more polar solvents should result in a higher reaction rate. Again, electron-donating ligands should enhance the catalyst activity due to their stabilizing effect on higher oxidation states of the ruthenium center, and sterically demanding ligands should facilitate the reductive elimination of the product. During the slow vinylidene formation step, the C(sp) proton is transferred to the ruthenium center. This proton may be detectable via ^{1}H NMR. When comparing the reactions of alkynes and 1-deuterioalkynes, a primary kinetic isotope effect is expected, as a C—D rather than a C—H bond has to be cleaved. The resulting product should be deuterated exclusively in the 1-position.

Caulton and co-workers investigated pathways leading to the formation of Ru—vinylidene intermediates.[33] They found that π-coordinated alkynes readily insert into Ru—H bonds to form Ru—vinyl complexes. The Ru—vinyl species then rearrange to Ru—H—vinylidene complexes. They isolated all postulated Ru intermediates and confirmed the pathways by DFT calculations. These showed reasonable energy barriers for the proposed pathway, and substantially higher barriers for an oxidative addition of the alkyne followed by a 1,3-proton shift. It is possible to incorporate this alternative route to vinylidene species into a new catalytic cycle for hydroamidations, which will further be referred to as *Mechanism D* (Scheme 6).

This catalytic cycle starts with the oxidative addition of an amide to an active Ru^0 species (**34**). After insertion of the alkyne into the Ru—hydride bond and rearrangement to the vinylidene species **39**, the amide attacks the carbon atom α to the ruthenium center, leading to the *anti*-Markovnikov enamide product (**6**—**13**) via reductive elimination. The oxidation state of the Ru center changes from 0 via +2 to +4 during the catalytic cycle, or only from 0 to +2 if the vinylidene ligand is interpreted as neutral carbene. The vinylidene formation proceeds without proton shifts, and at the end of the reaction, the alkyne proton is linked to the original C-atom.

For *Mechanism D*, a dependence of the reaction rate on the acidity of the N—H group of the amide as well as the C(sp)—H function of the alkyne should be detectable, resulting in measurable kinetic isotope effects both when *N*-deuterated amides or 1-[*D*]-alkynes are used as starting materials. Electron-rich ligands will stabilize the high oxidation state of the ruthenium center, and the use of sterically demanding ligands should facilitate the reductive elimination step. Reaction intermediates might be identifiable via ESI—MS and in situ IR experiments. It might also be interesting to investigate by in situ NMR whether the Ru-complexes are capable of activating N—H bonds.

In our previous work, we had excluded reaction mechanisms starting from Ru^0 species because no coupling product of the methylallyl ligands from the (cod)Ru(met)$_2$ precursor could be detected, and instead, free isobutene was observed via GC—MS and ^{1}H NMR spectroscopy, which appeared to support a redox-neutral ligand-exchange reaction.[29] A control experiment with 1-[*D*]-hex-1-yne showed no 1,2-proton shift during the reaction.[28] In situ NMR and ESI—MS experiments of the catalyst preformation step confirmed that all ligands of (cod)Ru(met)$_2$ are exchanged, and that cationic Ru-amide-phosphine and Ru-amide-phosphine-DMAP species are formed in the addition of secondary amides to terminal alkynes.[26] On the basis of these

Scheme 7. Redox-Neutral *Mechanism E* for the Hydroamidation of Terminal Alkynes
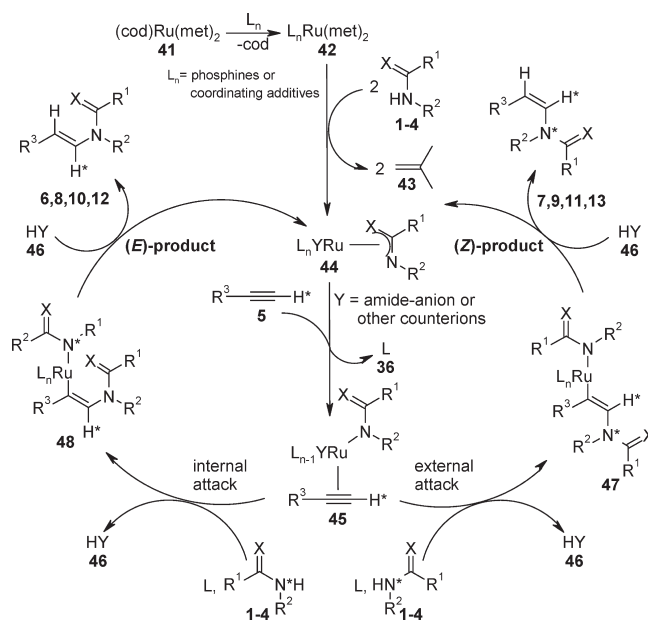
experiments, we postulated a redox-neutral ligand exchange mechanism, which will further be referred to as *Mechanism E* (Scheme 7).

In the catalyst preformation step, all ligands initially bound to the Ru-precursor are exchanged, with formation of ruthenium^{II}—amide complexes **44**. In the first step of the catalytic cycle, the alkyne coordinates to the ruthenium center (**45**). Depending on the steric bulk of the phosphines, the amide attacks from either the inner or the outer coordination resulting in the formation of *E*- or *Z*-configured enamides (**6**—**13**). Bulky ligands are likely to favor an external attack resulting in the formation of an (*E*)-Ru—enamide complex **47**, which releases the corresponding (*Z*)-enamide (**7**, **9**, **11**, or **13**) after protonolysis, along with a regenerated active Ru^{II}-species **44**. In contrast, an insertion of the alkyne into the Ru—N-bond of a coordinated amide is favorable in the presence of smaller ligands, giving rise to (*E*)-enamides (**6**, **8**, **10**, or **12**). Over the entire cycle, the Ru center remains in the oxidation state +2. A likely driving force behind the reaction is the continuous exchange of basic for more acidic ligands at the metal center.[34] *Mechanism E* offers an explanation for the stereochemistry of the hydroamidation, but cannot adequately address the limitation to terminal alkynes and selectivity for the *anti*-Markovnikov products.

If *Mechanism E* holds true, an inverse secondary kinetic isotope effect should be detectable for 1-deuterioalkynes, because it involves a rehybridization from sp to sp^2, which is more favorable for the stronger C—D bond.[35] Furthermore, no ruthenium—hydride species should be detectable via ^{1}H NMR. The nucleophilicity of the amide should have a strong influence on the reaction rate, and additives that increase the nucleophilic character of the amide should enhance the reaction rate. The ruthenium center remains in the oxidation state of +2 and merely activates the alkyne for nucleophilic attack by removing electron-density from the π-system. Therefore, less electron-rich phosphines should lead to a higher catalyst activity, whereas sterically demanding phosphines should lead to a reduced activity because the

Table 1. Overview of Experimental Findings for a Set of Control Experiments

Experimental finding	Expected outcome for *Mechanism*				
	A	*B*	*C*	*D*	*E*
1,2-proton shift in experiments with 1-[*D*]-alkynes	No	Yes	No	No	No
Primary kinetic isotope effect in hydroamidation competition experiments with 1-[*H/D*]-alkynes	No	Yes	Yes	Yes	No
Primary kinetic isotope effect in hydroamidation competition experiments with *N*-[*H/D*]-amides	Yes	Yes	Yes	Yes	Yes
Inverse secondary kinetic isotope effect in hydroamidation competition experiments with 1-[*H/D*]-alkynes	Yes	No	No	No	Yes
Detection of Ru-hydride species in ^{1}H-NMR hydroamidation experiments in absence of the alkyne	Yes	No	No	Yes	No
Detection of Ru-hydride species in ^{1}H-NMR hydroamidation experiments in absence of the amide	No	Yes	Yes	No	No
Detection of Ru-amide species in ESI-MS hydroamidation experiments in absence of the alkyne	Yes	No	No	Yes	Yes
Intermediacy of cationic species in the catalytic cycle	No	Yes	Yes	No	No

ligand-exchange reactions and the formation of the ruthenium—enamide intermediate are disfavored.

An overview of all predictions we made in this paragraph for *Mechanisms A—E* in a set of control experiments is presented in Table 1. These predictions are made under the assumption that the concentrations of all characteristic intermediates are high enough for detection and that the reaction steps leading to possible kinetic isotope effects (KIE) are slow.

All mechanisms presented above are in principle feasible, but give contradictory predictions for the outcome of simple control experiments and spectroscopic studies. The combined experimental findings presented herein provide strong evidence that the reaction proceeds via *Mechanism D*.

■ DEUTERATION STUDIES OF HYDROAMIDATIONS

We started our mechanistic investigation with hydroamidation experiments using 1-deuterioalkynes. *Mechanisms A, C, D*, and *E* predict that the deuterium should end up in the geminal position to the amide nitrogen, whereas *Mechanism B* predicts that the deuterium should be transferred to the vicinal carbon. In the inverse experiment, with *N*-deuterioamides and nondeuterated alkynes, the deuterium should be incorporated to the geminal position to the amide nitrogen for *Mechanism B* and bind to the vicinal atom for *Mechanisms A, C, D*, and *E*.

Deuteration studies were carried out for the additions of primary and secondary amides as well as imides, using both the *E*- and the *Z*-selective methods. The results are summarized in Table 2.

The addition of 2-pyrrolidone (**1a**) to 1-[*D*]-hex-1-yne (**5a**, Deuteration grade, DG = 92%) using the *E*-selective protocol (2 mol % (cod)Ru(met)$_2$, 6 mol % P(*n*-Bu)$_3$, 4 mol % DMAP) led to incorporation of the deuterium almost exclusively in the 1'-position of the corresponding enamide (**6aa**), that is, in geminal position to the amide (entry 1). The 2'-deuterated product (**6ab**) was detected in traces only. In the analogous reaction of 1-[*D*]-2-pyrrolidone (**1b**, DG = 85%) and 1-hexyne

(**5b**), the deuterium was transferred to the 2'-position of **6ab** in very high selectivity (entry 2). These results indicate that the predominant mechanism does not involve proton shifts. The trace formation of 2'-deuterated product can be accounted for by H—D exchange reactions at a relatively acidic site of the hydroamidation product, possible competing mechanisms, or unproductive vinylidene rearrangements.

The reaction of 2-pyrrolidone (**1a**) and 1-[*D*]-hex-1-yne (**5a**) under *Z*-selective conditions (2 mol % (cod)Ru(met)$_2$, 3 mol % Cy$_2$PCH$_2$PCy$_2$, 2 equiv H$_2$O) also proceeded mostly without proton shift (entry 3). The ratio between 2'-deuterated (**7ab**) versus 1'-deuterated product (**7aa**) dropped to a moderate value of 4:1 for the inversely deuterated starting materials (entry 4). In both reactions, the deuteration grades in the products were only moderate, which we attribute to the presence of water in the reaction mixture responsible for background H—D exchange reactions. Indeed, when we replaced the water, which is essential for an effective hydroamidation protocol, by deuterium oxide, the deuteration rates in the products (**7aa** and **7ab**) were high (entries 5 and 6). However, the regioselectivity of the deuteration was only moderate, and in the reaction of 1-[*D*]-hex-1-yne (**5a**), a doubly deuterated product was observed. All these findings suggest that background H—D exchange overlays regioselective deuterium incorporation in the presence of water.

The catalytic addition of succinimide (**2a**) to 1-[*D*]-hex-1-yne (**5a**) under *E*-selective conditions (5 mol % (cod)Ru(met)$_2$, 15 mol % P(*i*-Pr)$_3$, 4 mol % Sc(OTf)$_3$) proceeds without proton shift and leads exclusively to the incorporation of the deuterium in the 1'-position of the corresponding enimide product (**8aa**, entry 7). When using the inversely deuterated starting materials, the deuterium is mainly incorporated in the 2'-position of the enimide product (**8ab**, entry 8). In addition to the expected products, traces of the product deuterated in the α-position to the imide carbonyl group were detected, which can be rationalized by H/D exchange at this acidic position.[36]

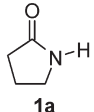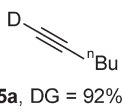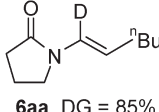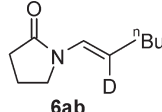**Table 2. Hydroamidation with Deuterated Starting Materials[a]**
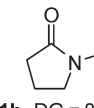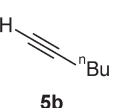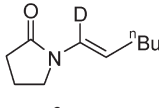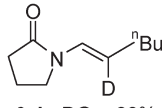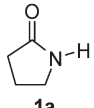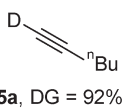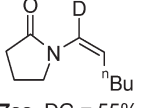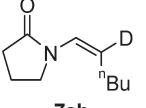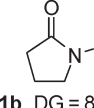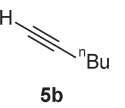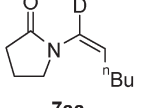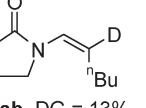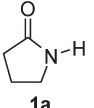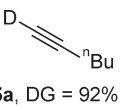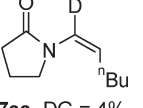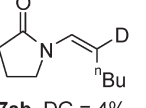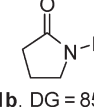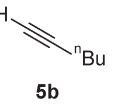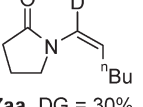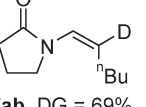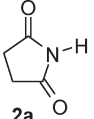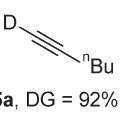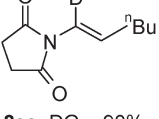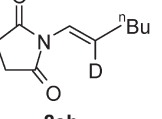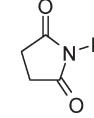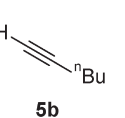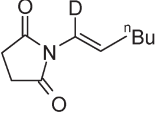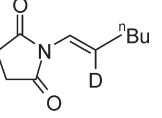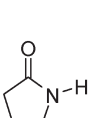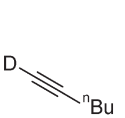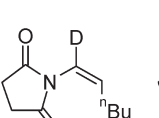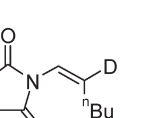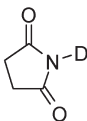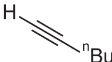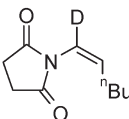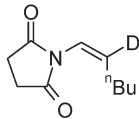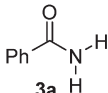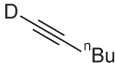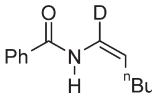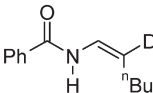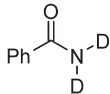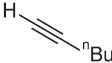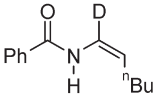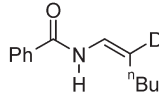
Entry	Amide	Alkyne	Products	Yield Ratio **6aa:6ab**
1	1a	5a, DG = 92%	6aa, DG = 85% / 6ab	92% / >30:1
2	1b, DG = 85%	5b	6aa / 6ab, DG = 80%	91% / <1:30
3[b]	1a	5a, DG = 92%	7aa, DG = 55% / 7ab	89% / 12:1
4[b]	1b, DG = 85%	5b	7aa / 7ab, DG = 13%	90% / 1:4
5[c]	1a	5a, DG = 92%	7aa, DG = 4% / 7ab, DG = 4%	80% / 1:1[d]
6[c]	1b, DG = 85%	5b	7aa, DG = 30% / 7ab, DG = 69%	91% / 1:2
7[e]	2a	5a, DG = 92%	8aa, DG = 90% / 8ab	75% / >30:1
8[e,f]	2b, DG = 81%	5b	8aa / 8ab, DG = 56%	92% / <1:30[g]
9[h]	2a	5a, DG = 92%	9aa, DG = 84% / 9ab	92% / >30:1

Table 2. Continued

Entry	Amide	Alkyne	Products	Yield Ratio **6aa:6ab**
10[h]	**2b**, DG = 81%	**5b**	**9aa** **9ab**, DG = 83%	91% <1:30[g]
11[i]	**3a**	**5a**, DG = 92%	**10aa**, DG = 87% **10ab**	89% >30:1
12[i]	**3b**, DG = 75%	**5b**	**10aa** **10ab**, DG = 62%	87% <1:30

[a] *Reaction conditions*: Amide or imide (1.00 mmol), alkyne (2.00 mmol), (cod)Ru(met)$_2$ (2 mol %), P(n-Bu)$_3$ (6 mol %), DMAP (4 mol %), toluene (3 mL), 100 °C, 15 h, selectivity determined by ^{1}H NMR; DG = deuteration grade. [b] Cy$_2$PCH$_2$PCy$_2$ (3 mol %) instead of P(n-Bu)$_3$, H$_2$O (2.00 equiv) instead of DMAP. [c] Cy$_2$PCH$_2$PCy$_2$ (3 mol %) instead of P(n-Bu)$_3$, D$_2$O (2.00 equiv) instead of DMAP. [d] The doubly deuterated product was mainly formed with a DG of 91%. [e] (cod)Ru(met)$_2$ (5 mol %), P(i-Pr)$_3$ (15 mol %), Sc(OTf)$_3$ (4 mol %), DMF-d_7 (3 mL), 60 °C, 15 h, isolated yields, selectivities determined by ^{1}H NMR. [f] DMF (3 mL) instead of DMF-d_7. [g] A product deuterated in the 3-position of the imide was detected in traces. [h] (cod)Ru(met)$_2$ (2 mol %), P(n-Bu)$_3$ (6 mol %), Sc(OTf)$_3$ (4 mol %), DMF (3 mL), 60 °C, 15 h, isolated yields, selectivities determined by ^{1}H NMR. [i] (cod)Ru(met)$_2$ (5 mol %), dcypb (6 mol %), Yb(OTf)$_3$ (4 mol %), DMF (3 mL), 60 °C, 6 h, isolated yields, selectivity determined by ^{1}H NMR.

Similar results were observed also for the *Z*-selective protocol (2 mol % (cod)Ru(met)$_2$, 6 mol % P(n-Bu)$_3$, 4 mol % Sc-(OTf)$_3$). Thus, the reaction of succinimide (**2a**) with 1-[*D*]-hex-1-yne (**5a**) yielded the enimide mainly deuterated in the 1′-position (**9aa**, entry 9), whereas the addition of *N*-[*D*]-succinimide (**2b**, DG = 81%) to 1-hexyne (**5b**) led to the formation of the product with near-quantitative deuterium incorporation in the 2′-position (**9ab**, entry 10). The hydroamidation therefore also proceeded without proton shift, as did the reaction of the secondary amides **1a** and **1b**.

The reaction of benzamide (**3a**) with 1-[*D*]-hex-1-yne (**5a**) under *Z*-selective conditions (5 mol % (cod)Ru(met)$_2$, 6 mol % dcypb, 4 mol % Yb(OTf)$_3$) furnished the corresponding enamide **10aa** deuterated exclusively in the 1′-position (entry 11). Analogously, the deuterium was selectively incorporated in the reaction of *N,N*-[*D*$_2$]-benzamide (**3b**, DG = 75%) and 1-hexyne (**5b**) under otherwise identical conditions (**10ab**, entry 12). It is worth mentioning that, in contrast to the previously reported hydroamidation protocol for the addition of primary amides,[29] we had to perform these two deuteration experiments without water, because in the presence of water H−D exchange reactions overlaid regioselective deuterium incorporation.

On the basis of these results, the formation of vinylidene intermediates via a 1,2-proton shift or via oxidative addition of the alkyne followed by a 1,3-proton shift as postulated in *Mechanism B* can be ruled out for both *E*- and *Z*-selective hydroamidation reactions. *Mechanisms A, C, D*, and *E* are all in agreement with the results of the present deuteration studies.

■ KINETIC INVESTIGATIONS OF HYDROAMIDATIONS

We next investigated the kinetics of hydroamidations by means of in situ IR spectroscopy. Using a ReactIR 45 m FT-IR spectrometer (3.2 scans/s, 8 cm^{-1} resolution), we monitored the hydroamidation of 2-pyrrolidinone (**1a**) and 1-hexyne (**5b**) by the disappearance of the C−C triple bond valence oscillation of 1-hexyne (**5b**) at 2122 cm^{-1} and the appearance of a C=O valence oscillation of the enamide product (**6a**) at 1725 cm^{-1}. Figure 3 illustrates the starting material consumption as well as the product formation and the temperature inside the reaction vessel over a period of 30 min. The reaction starts almost immediately after the reaction vessel is placed in an aluminum block preheated to 100 °C and is complete within several minutes.

Evaluation of the spectroscopic data with the iC IR software using the ConcIRT algorithm also allowed to detect the appearance of short-lived reaction intermediates by their C=C vibration stretches at 1607 cm^{-1} (see Supporting Information). This frequency is in an area typical for ruthenium–vinylidene species.[37] However, in-depth studies under carefully optimized conditions would be required to unambiguously confirm these species.

Attempts to slow down the reaction by lowering the temperature were unsuccessful. Below 100 °C, the hydroamidation was sluggish, and undesired alkyne dimerization became the predominant process. Even at the optimum reaction temperature, the catalyst preformation did not always proceed at the same speed, so that the variability of overall reaction rates was rather high.

It was therefore unfeasible to perform comparative kinetic studies with deuterated and nondeuterated substrates in separate vessels to determine kinetic isotope effects. Instead, we performed
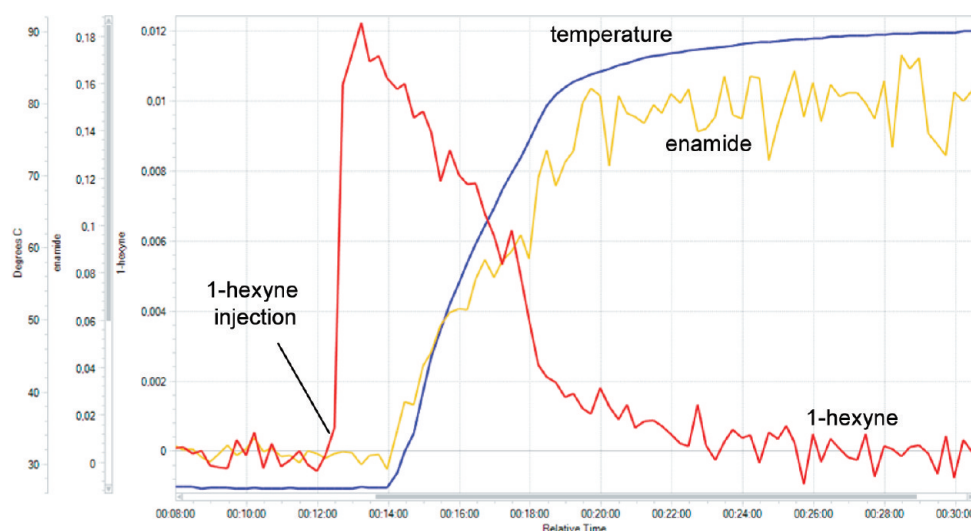
Figure 3. In situ IR-experiment: Concentration trends for the hydroamidation of 1-hexyne (**5b**) with 2-pyrrolidinone (**1a**).

competition experiments in which one of the starting materials was added in large excess as a 1:1 mixture of its deuterated and nondeuterated form (Table 3). From the ratio of hydrogen versus deuterium incorporation in the enamide product, we calculated the relative reaction rates.

In the reaction of 2-pyrrolidinone (**1a**) with 1-hexyne (4 equiv, DG adjusted to 50%), the enamide (**6a/6aa**) was obtained with a DG of 39% (entry 1). This translates to a kinetic isotope effect (KIE) of 1.6. Similarly, the reaction of succinimide (**2a**) with 1-hexyne (4 equiv, DG adjusted to 50%) gave a product (**9a/9aa**) with 30% DG, translating to a KIE of 2.3 (entry 2). In the analogous reaction of benzamide (**3a**), the product DG was 40% (**10a/10aa**), corresponding to a KIE of 1.5 (entry 3).

In all cases, normal kinetic isotope effects (KIE = $k_H/k_D = n_H/n_D$) greater than 1 were observed. During the reaction, the hybridization of the C(1) carbon changes from sp to sp^2 and any intermediate should thus have a higher or the same p-character as the starting material. However, a reaction step during which the p-character of a C−H bond increases is known to lead to an inverse secondary KIE. Thus, the KIE should always have a value smaller than 1, unless the sp C−H bond is cleaved in a slow reaction step, and a sp^2 C−H bond is reinstated at the same carbon atom in a later, non rate-determining step.[35] This implies that, despite their relatively small magnitudes, the values must result from a primary KIE. *Mechanism A*, which does not involve a bond cleavage but rather an insertion of the alkyne into a Ru−H or Ru−N bond with sp to sp^2 rehybridization, can thus be excluded as the main reaction pathway. *Mechanism E* is also incompatible with the observed KIE > 1, as in this process, the C−H bond is also not cleaved.

In *Mechanisms C* and *D*, a rearrangement step from a ruthenium−vinyl to a ruthenium−hydride−vinylidene species takes place, during which the C(sp)−H/D bond is cleaved. The KIE values greater than 1 are in good agreement with these pathways. Although primary KIEs for deprotonation processes usually have values of 4−7, the relatively low values of 1.5−2.3 observed here are easily rationalized when considering that the overall catalytic process consists of several steps. For example, if one reaction step is slower by a factor of 5 because of an isotope effect, but this individual reaction step requires only one-forth of the catalyst turnover time, the overall KIE would be 2 rather than 5.

Table 3. Determination of KIE Values by Competition Experiments[a]
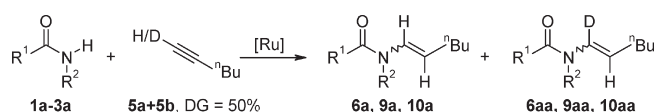
Entry	Amide	Main Product	Ratio **a/aa**	KIE[b]
1	**1a**	DG = 39%, **6a/6aa**	1.6:1	1.6
2[c]	**2a**	DG = 31%, **9a/9aa**	2.3:1	2.3
3[d]	**3a**	DG = 40%, **10a/10aa**	1.5:1	1.5

[a] *Reaction conditions*: Amide (1.00 mmol), 1-hexyne (2.00 mmol), 1-[*D*]-hex-1-yne (2.00 mmol), (cod)Ru(met)$_2$ (2 mol %), P(*n*-Bu)$_3$ (6 mol %), DMAP (4 mol %), toluene (3 mL), 100 °C, 15 h, product ratio determined by ^{1}H NMR. [b] Determined by the ratio of nondeuterated to deuterated product yields. [c] Sc(OTf)$_3$ (4 mol %) instead of DMAP, DMF (3 mL) instead of toluene, 60 °C, 15 h. [d] (cod)Ru(met)$_2$ (5 mol %), dcypb (6 mol %), Yb(OTf)$_3$ (4 mol %), DMF (3 mL), 60 °C, 6 h.

Indeed, in the reaction of 2-pyrrolidinone (4 equiv, DG adjusted to 50%) and hex-1-yne (**5b**) (Scheme 8), the enamide (**6a/6ab**) was obtained with a DG of 30%, translating to a KIE of 2.3. The fact that a noticeable KIE is again observed reveals that this step is also relatively slow. The KIE value for each individual step is thus probably larger than 4, resulting in a smaller observed KIE for the overall reaction because the catalytic cycle involves at least two slow steps.

Scheme 8. Competition Hydroamidation Experiment with 1-[D]-2-Pyrrolidinone (1b)
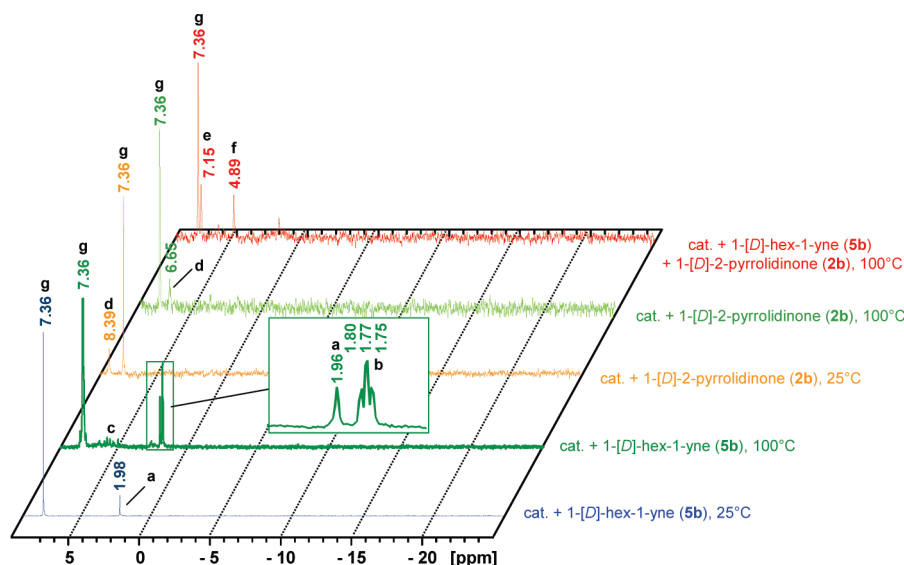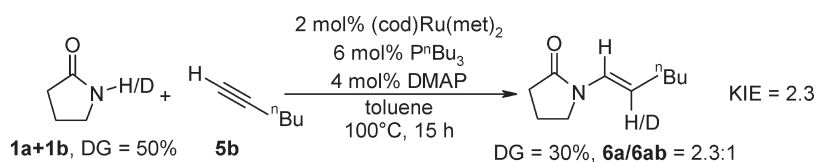
Figure 4. In situ ^{2}H NMR experiments with 1-[D]-hex-1-yne (**5b**) and 1-[D]-2-pyrrolidinone (**1b**). (a) Free 1-[D]-hex-1-yne; (b) triplet signal; (c) oligomerization products; (d) free 1-[D]-2-pyrrolidinone; (e) 1′-deuterium of the enamide; (f) 2′-deuterium of the enamide; (g) benzene-d_6.

Another possible explanation for the relatively small values is that the transition state is a nonlinear one.[38]

Overall, only *Mechanisms C* and *D*, both involving Ru–vinylidene intermediates formed without proton shifts, are in agreement with the outcome of both the deuteration studies and the kinetic investigations.

■ NMR STUDIES OF HYDROAMIDATIONS

We next performed in situ NMR studies with the goal of identifying potential Ru-bound organic fragments. However, the reaction proceeds very rapidly when using increased amounts of Ru catalyst, and the spectra contained numerous signals pertaining to ligands, additives, and byproducts that often obscured relevant species. To specifically monitor species derived from the alkyne and amide starting materials, we used deuterated derivatives and followed the reaction by ^{2}H NMR. This greatly simplified the NMR spectra obtained (Figure 4). Unfortunately, the sensitivity of this spectroscopic method was determined to be rather low.

^{2}H NMR spectra of a mixture containing the catalyst (20 mol % (cod)Ru(met)$_2$, 60 mol % P(n-Bu)$_3$, 40 mol % DMAP) and 1-[D]-hex-1-yne (**5a**) only were recorded in toluene, using benzene-d_6 as an internal standard (Figure 4 and Supporting Information).

At room temperature, only the signal pertaining to the starting material was visible (a), confirming that the catalyst activation requires elevated temperatures. Indeed, at 100 °C, a new broad triplet (b) was detected at δ = 1.77 ppm (J = 2.2 Hz). Moreover, a series of signals in the range of 4.89–6.20 ppm (c) rapidly appeared and increased in intensity with concomitant consumption of the

alkyne, which can be attributed to alkyne oligomerization products. Some of them might also originate from Ru–vinyl species, but an unambiguous assignment of signals to such intermediates was not possible. When both 1-[D]-hex-1-yne (**5b**) and 2-pyrrolidinone (**1a**) were present, the same triplet (b) was detected along with a strong signal for the C(1)-deuterated enamide product (e). Alkyne oligomerization products (c) and C(2)-deuterated enamide (f) were detected only in traces.

This triplet (b) was not in good agreement with literature NMR data for ruthenium alkyne and vinyl complexes (Figure 5). Terminal protons of coordinated alkynes should appear around 5 ppm and have a large H–P coupling.[39] Ru–H and Ru–vinyl species should also appear at chemical shifts different than 1.77 ppm.[33] Considering the small value of D–H couplings in ^{2}H NMR spectra[40] and the broad shape of triplet b, this signal might be assigned to the vinylic proton of a Ru–vinylidene–phosphine species. For a known *trans*-[(dppm)$_2$(Cl)Ru=C=CH^{n}Bu]PF$_6$ complex (dppe = bisdiphenylphosphino methane) with the identical 1-hexyne-derived vinylidene ligand, Dixneuf et al. reported a triplet of quintets at 2.5 ppm in the ^{1}H NMR spectrum (Figure 5).[41] Coupling constants of 7.9 and 2.8 Hz for the vinylic proton at the vinylidene entity could be determined, resulting from a coupling to two neighboring protons and a long-range coupling to four phosphine atoms. The chemical shift of triplet b is in good range for such a vinylic proton, considering that the Ru center should be more electron-rich because of the stronger donor capacity of alkyl phosphine compared with the aryl phosphine ligands. That should lead to an upfield shift of the proton signal. The observed coupling constant of 2.2 Hz is in agreement with a long-range

-11.3 (t, J_{P-H} = 29.8 Hz, Ru-H)
99.8 (s)

5.3 (dd, J_{P-H} = 18.3 Hz,
J_{P-H} = 1.8 Hz)
7.6 (s), 4.2 (s)

6.1 (dt, J_{H-H} = 21.0 Hz, J_{H-H} = 2.1 Hz)
8.1 (dt, J_{H-H} = 21.0 Hz, J_{H-H} = 1.6 Hz)
43.7 (s)

δ (^{1}H-NMR)
δ (^{31}P{H}-NMR)

-12.7 (t, J_{P-H} = 17.8 Hz, Ru-H)
4.4 (t, J_{P-H} = 3.4 Hz, C=CHPh)
42.7 (s)

-15.0 (dt, J_{P-H} = 18.3 Hz,
J_{H-H} = 1.8 Hz, Ru-H)
2.6 (dt, J_{P-H} = 3.6 Hz,
J_{H-H} = 1.8 Hz, C=CHSi).
40.3 (s)

2.5 (t, quint, J_{H-H} = 7.9 Hz,
J_{P-H} = 2.8 Hz, C=CH^{n}Bu)
-15.3 (s)
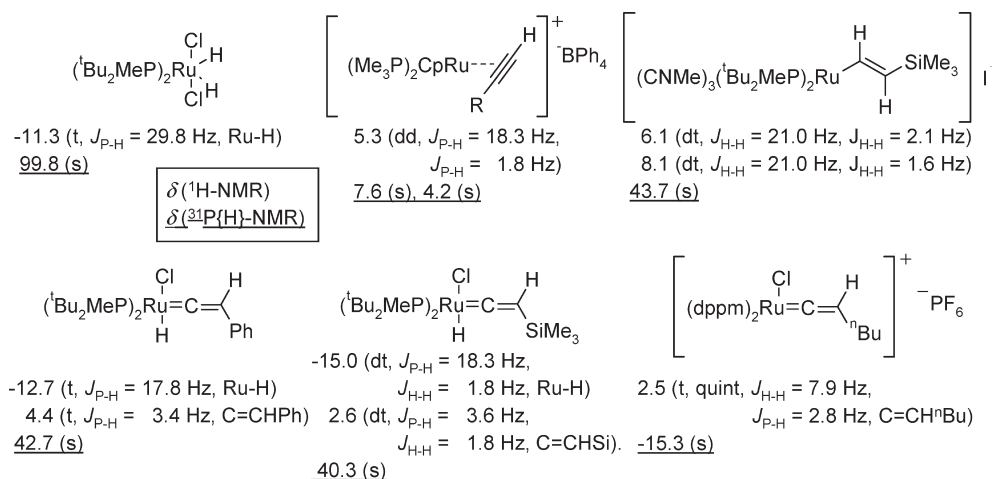
Figure 5. ^{1}H- and ^{31}P NMR chemical shifts for selected ruthenium–phosphine complexes.
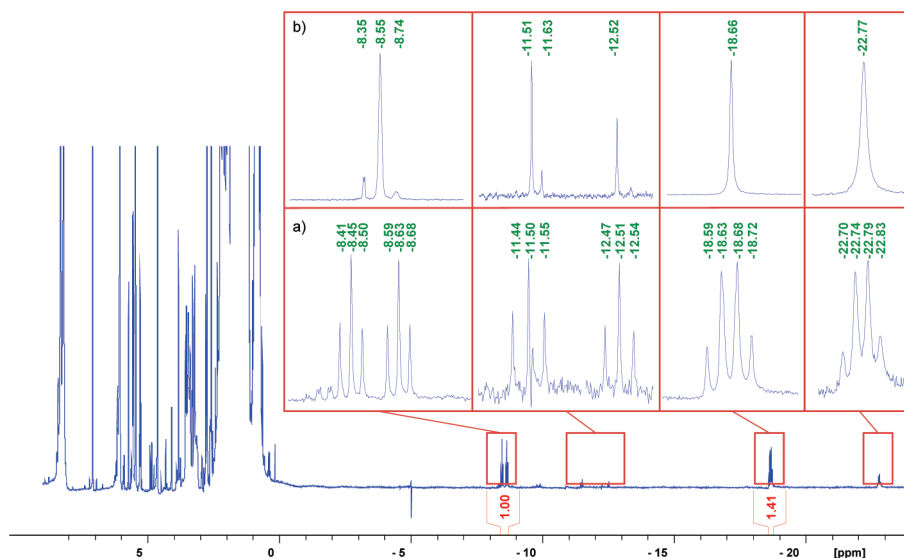
Figure 6. In situ ^{1}H NMR experiments with 2-pyrrolidinone (**1a**) at ambient temperature after heating to 100 °C for 5 min. (a) ^{1}H NMR experiment; (b) ^{1}H{^{31}P}-NMR experiment.

coupling to two phosphine atoms. The broad shape might indicate that the coupling to the neighboring protons, which is expected to be arround 1 Hz for such a D—H coupling,[40] could not be resolved in this in situ ^{2}H NMR experiment. These results suggest that, in the absence of the amide, a Ru—vinylidene species is formed, possibly via 1,2-proton shift. This is in agreement with the observation by Dixneuf that alkyne oligomerization reactions proceed via vinylidene species.[32,42]

In an attempt to find evidence for Ru—H species resulting from the oxidative addition of amides, we recorded the ^{2}H NMR spectrum for a mixture of 1-[D]-2-pyrrolidinone (**1b**) with the catalyst system (40 mol % (cod)Ru(met)$_2$, 120 mol % P(n-Bu)$_3$, 80 mol % DMAP) in toluene using benzene-d_6 as an internal standard (Figure 4). However, it contained only the signal for the free amide (d). Subsequent addition of 1-[D]-hex-1-yne (**5a**) led to a rapid disappearance of this signal with concomitant appearance of the signals for vinylic deuterium atoms of the enamide product (e and f). The reaction simply proceeded too rapidly to allow a detection of any intermediates by ^{2}H NMR.

We next investigated the reaction mixtures with the help of ^{1}H NMR, as this is more sensitive than ^{2}H NMR. In the ^{1}H NMR spectrum of a mixture containing the catalyst (20 mol % (cod)Ru(met)$_2$, 60 mol % P(n-Bu)$_3$, 40 mol % DMAP) and 1-hexyne (**5b**) but no amide (see Supporting Information), multiple signals in the range of 4.66–6.12 ppm were observed, but none were detected below 0 ppm in the region characteristic for Ru—H species. Such signals would have been expected for *Mechanisms B* and *C*. A corresponding signal for triplet b observed in the ^{2}H NMR experiment at 1.77 ppm could not be found in the ^{1}H NMR spectrum since the area from 0 to 3 ppm was overlaid with multiple broad proton signals of alkyl groups, for example, from the phosphine ligands.

In contrast, after briefly heating a mixture of the catalyst and 2-pyrrolidinone (**1a**) to 100 °C, the ^{1}H NMR spectrum showed several new signals below 0 ppm (Figure 6): A group of peaks consisting of a duplet of triplets, two triplets and two quartets appeared between −8 and −23 ppm with coupling constants between 22 and 33 Hz for the triplets and quartets and 108 Hz for
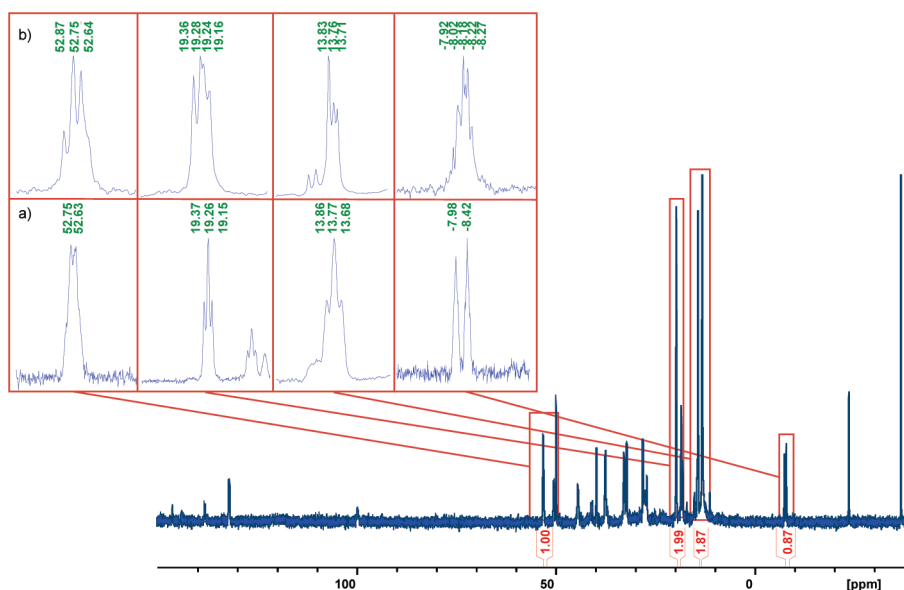
Figure 7. In situ ^{31}P NMR experiments with 2-pyrrolidinone (**1a**) measured at 22 °C after heating to 100 °C for 5 min. (a) ^{31}P NMR experiment; (b) ^{31}P{^{1}H}-NMR experiment.
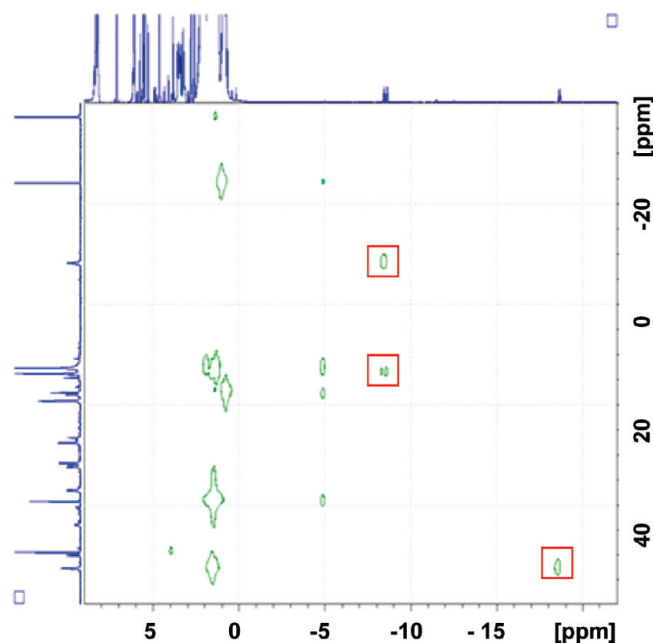
Figure 8. In situ H,P-HMQC experiments with 2-pyrrolidinone (**1a**) at ambient temperature after heating to 100 °C for five minutes.

Figure 9. In situ P,P-COSY experiments with 2-pyrrolidinone (**1a**) at ambient temperature after heating to 100 °C for 5 min.

the duplet. Because of the extreme upfield shift of these signals, they are likely to originate from Ru—H species.[33] Coupling constants of 20—30 Hz are typical for *cis* H—Ru—P couplings in ruthenium hydride species stabilized by phosphines. The observed coupling constants of 108 Hz are in the expected range for *trans* H—Ru—P coupling in such complexes.[43] That the observed couplings indeed resulted from H—Ru—P interactions could be verified by phosphorus-decoupled ^{1}H NMR experiments with the same sample. Here, all signals changed to singlets.

The ^{31}P-spectrum revealed that many different phosphine species are present in the reaction mixture (Figure 7). Only the

signal at −37.26 ppm could unambiguously be assigned to free tri-*n*-butylphosphine.

H,P-HMQC (Heteronuclear Multiple Quantum Coherence) and P,P-COSY (Correlation spectroscopy) experiments were used to elucidate which of these phosphine signals correspond to the Ru—H species (Figures 8 and 9).

The intensity of the proton signals at −8.55 and −18.66 ppm species was sufficient to detect them in the 2D NMR experiments. The H,P-HMQC (Figure 8) showed cross-peaks between the Ru—H-signal at −8.55 and phosphorus signals at −8.20 ppm and 13.77 ppm, which are in a reasonable range for Ru-coordinated phosphines. The signal at −8.20 ppm integrates as

Scheme 9. In Situ Formation of Ru—H-Phosphine Complexes Starting from (Cod)Ru(met)$_2$ and the Resulting ^{1}H-NMR Coupling Patterns
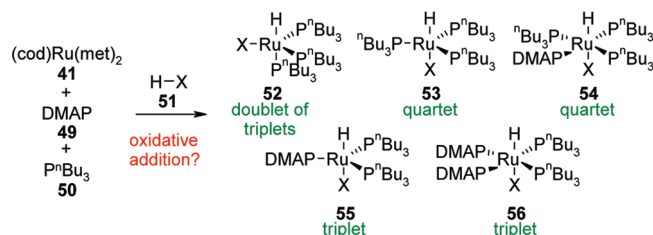
one, the signal at 13.77 ppm as two P-atoms in the ^{31}P- spectrum. In the P,P-COSY spectrum (Figure 9), a cross-peak between the two phosphorus signals is observed, confirming that all signals belong to a single Ru-species likely to contain one hydride and three phosphine ligands. The best interpretation for the H—P coupling constants for the proton signal at −8.55 ppm ($J_{H-P} = 27$ and 108 Hz) is that two of the phosphines are in *cis*- and one is in *trans*-position to the Ru—H bond (Scheme 9, **52**).

The H,P-HMQC (Figure 8) also showed a cross-peak for the proton signal at −18.66 ppm and the phosphorus signal at 52.69 ppm. A quartet was observed for this proton in the ^{1}H NMR which merged to a singlet in the P-decoupled ^{1}H NMR spectrum. In addition, the P,P-COSY (Figure 9) showed a clear cross-peak between the phosphorus signals at 52.69 and 19.26 ppm. The signal at 52.69 ppm integrates as one P-atom, and the signal at 19.26 ppm as two P-atoms in the ^{31}P- spectrum. These combined findings indicate an octahedral Ru-species with three phosphine ligands and one DMAP ligand in plane (Scheme 9, **54**). Two phosphorus signals are expected for species **54**, one for the two P-atoms next to, and one for the P-atom in *trans* position to the DMAP ligand. Therefore, the observed quartet in the ^{1}H NMR spectrum must actually be a duplet of triplets with nearly identical *cis* H—P couplings, which leads to an overlay of two triplets to one quartet.

The remaining upfield signals in the ^{1}H NMR showed very similar splitting patterns that disappear in the P-decoupled proton spectrum and are also likely to originate from Ru—H phosphine complexes. Beside the duplet of triplets at −8.55 ppm and the pseudo quartet at −18.66 ppm, two triplets at −11.50 and −12.51 ppm and one quartet at −22.77 ppm were detected in the ^{1}H NMR. Their coupling patterns and coupling constants in the range of 24−36 Hz also suggest Ru—H—phosphine complexes with, respectively, two and three phosphines coordinated in *cis*-position to the hydride. Scheme 9 provides for an overview of possible Ru—H species that would be in agreement with the spectroscopic data obtained.

We next added phenylacetylene-2-^{13}C (**5c**) to the NMR sample containing 2-pyrrolidinone (**1a**), 40 mol % (cod)Ru(met)$_2$, 120 mol % P(*n*-Bu)$_3$, 80 mol % DMAP and toluene-d_8 which had shown the signals for Ru—H species, and performed further ^{13}C- and ^{1}H NMR experiments (see Supporting Information).

The proton-decoupled ^{13}C NMR spectrum showed multiple signals below 200 ppm. A triplet detected at 214 ppm and a duplet of duplets of duplets at 216 ppm seemed to originate from Ru—alkyne intermediates, since no signals of an organic fragment should appear at chemical shifts higher than 200 ppm.

It is not straightforward to assign these signals. The coupling constants between 8 and 28 Hz seem to result from

carbon−Ru−phosphorus couplings. However, Ru−vinylidene species should appear at chemical shifts higher than 300 ppm, Ru−vinyl species between 120 and 170 ppm, and Ru−alkyne π-complexes around 75 ppm.[44]

The corresponding ^{1}H NMR spectrum showed a duplet of triplets at around −7.4 ppm and a duplet of triplets of duplets at around −8.7 ppm. Before the addition of phenylacetylene-2-^{13}C (**5c**), the signal at −8.7 ppm appeared as a duplet of triplets with H−P couplings of 108 and 27 Hz, whereas after the addition of phenylacetylene-2-^{13}C (**5c**), the H−P couplings changed in part to 87 and 27 Hz and an additional coupling of 7 Hz appeared which must result from a proton-carbon coupling. The H−C coupling might originate from a π-coordination of phenylacetylene-2-^{13}C (**5c**) to species **52** (Scheme 9), the formation of a Ru−vinylidene−hydride such as **29** and **39**, or a Ru−hydride−enamide species such as **31** and **40**.

After heating the reaction mixture briefly to 100 °C, the spectra revealed that the reaction was already complete, as expected for this highly reactive alkyne.

We continued our in situ NMR studies with the investigation of the *Z*-selective hydroamidation of secondary amides (see Supporting Information). The first generation catalyst system for the *Z*-selective hydroamidation of secondary amides proved to be unsuitable for NMR investigations because of the high amount of water (8 equiv) required for this catalyst system,[25] causing massive solubility problems and preventing an effective shimming during the measurements. Therefore, we used a modified protocol of the second generation catalyst system.[30] The experiments were performed in DMF-d_7 instead of chlorobenzene and the paramagnetic Yb(OTf)$_3$ was substituted by diamagnetic Sc(OTf)$_3$. Because of the high catalyst loading (40 mol % (cod)Ru(met)$_2$, 45 mol % dcypb, 80 mol % Sc(OTf)$_3$, 2-pyrrolidinone (**1a**), DMF-d_7) only broad signals were detected in the ^{1}H NMR spectrum. After centrifugation of the suspension in the NMR tube and briefly heating to 100 °C, the ^{1}H NMR spectrum showed several signals between −15 and −25 ppm. These signals below 0 ppm confirm the formation of Ru−hydride species under *Z*-selective reaction conditions, indicating a similar reaction mode for this protocol. Unfortunately, no characteristic H−P couplings could be determined. The corresponding ^{31}P NMR spectrum showed several low intensity phosphorus signals between −20 and 70 ppm.

The results from these NMR studies strongly suggest that Ru−H−phosphine complexes are present in the reaction mixtures of hydroamidation reactions. The experiments also show how readily Ru−H species are formed when an amide is added to a Ru−phosphine catalyst, presumably via oxidative insertion into the N−H bond.[19,22,45] These observations, in combination with the findings of Caulton et al., who reported that Ru−H-complexes rapidly react with alkynes under formation first of Ru−vinyl and then of Ru−vinylidene complexes,[33] all point in the direction of *Mechanism D*. After all, *Mechanisms A* and *D* are the only ones that involve Ru−H species formed via an oxidative addition of N−H nucleophiles. In *Mechanisms E*, Ru−H species are not involved at all and can be ruled out. In *Mechanisms B* and *C*, Ru−H species are formed in the reaction of a Ru-precursor with an alkyne without participation of the amide. However, in the NMR experiments, the fact that Ru−H species were observed in the presence of amide but not in the presence of alkyne contributes to the evidence against *Mechanisms B* and *C*. Considering that the results of the labeling experiments and the kinetic studies are incompatible with
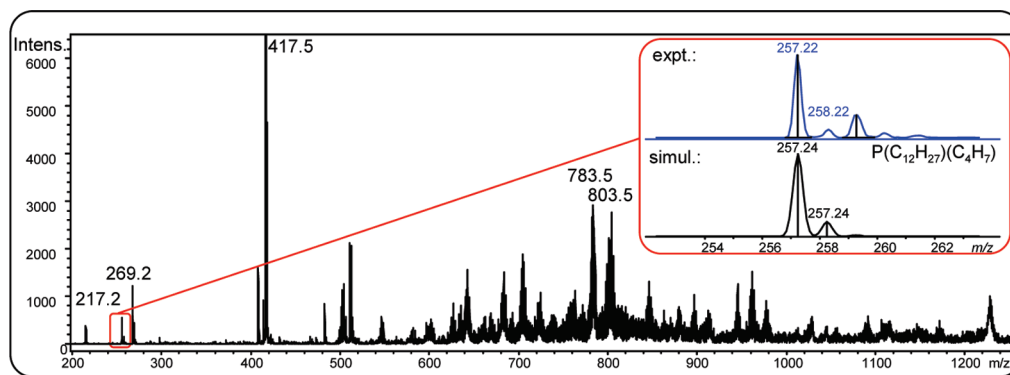
Figure 10. Assignment of $[(n\text{-Bu})_3P{-}C_4H_7]^+$ (m/z = 257.2) as the product of an allylic substitution reaction of methylallyl ligands with tri-*n*-butylphosphine.

Mechanisms A, B, and *E, Mechanism D* at this stage appears to be most likely.

■ IN SITU ESI−MS EXPERIMENTS

The electronspray ionization mass spectroscopy (ESI−MS) has evolved as a key technology in the investigation of reaction mechanism. In pioneering work, Chen et al., for example, used ESI−MS to identify key intermediates for the Ru-catalyzed olefin metathesis,[46] and Pfaltz et al. and di Lena et al. used ESI−MS technology to develop more efficient and more selective catalyst systems.[47] Intrigued by the predictive power of these investigations, we performed a series of in situ ESI−MS experiments with the goals of investigating the catalyst preformation step and identifying reaction intermediates that further support any of the proposed catalytic cycles.

There is ample literature evidence that the cod ligand is immediately replaced by more strongly coordinating phosphine and/or DMAP ligands, giving rise to a $L_nRu(met)_2$ species (L = phosphine, DMAP).[26,29] To differentiate between the proposed mechanisms, the decisive question to be addressed is whether the methylallyl ligands remain bound to Ru^{II} (consistent with *Mechanisms B* and *C*), become protonated and replaced by another ligand (consistent with *Mechanisms B, C* and *E*), or are cleaved via a reductive elimination step leading to Ru^0 species (consistent with *Mechanisms A* and *D*).

In this context, we investigated several combinations of $(cod)Ru(met)_2$, $P(n\text{-Bu})_3$ and DMAP by ESI−MS, both at room temperature and after briefly heating to 100 °C. The spectra obtained at room temperature from all possible solutions showed low overall intensities and no clear assignment to Ru-species was possible (see Supporting Information). This is not surprising, as the expected neutral Ru(II) complexes with strongly coordinating counterions would be hard to detect. However, after briefly heating the solutions to 100 °C, the overall intensities increased and clear signals for Ru^{II} species could be detected in all cases, except for the toluene solution of $(cod)Ru(met)_2$ alone.

The solution of $(cod)Ru(met)_2$ and DMAP showed three signals at m/z = 371.1, 625.2, and 716.3 which could only be matched with the calculated pattern for $[Ru(met)(DMAP)(tol)]^+$ (met = $C_4H_7{}^-$, DMAP = $C_7H_{10}N_2$, tol = toluene, C_7H_8), $[Ru(met)_2(cod\text{-}H_2)(DMAP)(tol)_2] + H^+$ (cod-H_2 = C_8H_{10}) and $[Ru(met)_2(cod\text{-}H_2)(DMAP)(tol)_3]^+$, illustrating that DMAP indeed coordinates to the Ru center and is able to replace the cod ligand. The dehydrogenation of the cod ligand leading to

cyclooctatriene (C_8H_{10}) or anionic cyclooctadienyl fragments ($C_8H_{10}{}^{2-}$) provides a simple explanation for the observed signal patterns. During the electrospray process, several toluene molecules seemed to condense to the detected cationic Ru-fragments. Such species are highly unstable and unlikely to exist in the reaction solution in significant abundances.

For the toluene solution of $P(n\text{-Bu})_3$ and $(cod)Ru(met)_2$, three signals of Ru species at m/z = 505.3, 761.5, and 779.5 were detected matching the calculated patterns of $[Ru(cod)(P(n\text{-Bu})_3)(tol)\text{-}(H)]^+$ ($P(n\text{-Bu})_3 = PC_{12}H_{27}$), $[Ru(met)(cod)(P(n\text{-Bu})_3)_2(tol)]^+$ and $[Ru(cod)(P(n\text{-Bu})_3)(tol)_4)] + H^+$.

For the toluene solution of $(cod)Ru(met)_2$, $P(n\text{-Bu})_3$ and DMAP, two strong signals at m/z = 783.5 and 803.5 were detected, that matched the calculated patterns for $[Ru(P(n\text{-Bu})_3)_2(tol)_3\text{-}(H)]^+$ and $[Ru(P(n\text{-Bu})_3)_3(tol)(H)_2] + H^+$.

Whenever $P(n\text{-Bu})_3$ was present the reaction solution, a series of three signals at m/z = 217.2, 257.2, and 417.5 was detected matching the calculated patterns of $[OPC_{12}H_{26}]^+$, $[(n\text{-Bu})_3P{-}C_4H_7]^+$ and $[O(PC_{12}H_{26})_2]^+$ fragments (Figure 10). The signals for $[OPC_{12}H_{26}]^+$ and $[O(PC_{12}H_{26})_2]^+$ fragments might have been caused by partial oxidation of $P(n\text{-Bu})_3$, but $[(n\text{-Bu})_3P{-}C_4H_7]^+$ fragment must be seen as evidence for a reduction process at the Ru center, in which a phosphine reacts with a methylallyl ligand with formation of a phosphonium salt that can be further deprotonated to the corresponding phosphorus ylide species $((n\text{-Bu})_3P{=}CH(C_3H_5))$. This coupling is known to occur in the reaction of bis(2-methylallyl)palladium chloride dimer with phosphines giving rise to $Pd^0{-}$phosphine complexes such as $Pd(P(n\text{-Bu})_3)_4$.[48]

This suggests that during catalyst preformation, the nucleophilic $P(n\text{-Bu})_3$ attacks one of the methylallyl ligands with formation of a phosphonium salt. In this process, Ru^{II} is reduced to Ru^0 while the second methylallyl ligand is protonated, for example, by the acidic proton of the phosphonium salt, with formation of isobutene. The resulting phosphorus ylide species are known to decompose to the corresponding phosphine oxide and the alkene. Indeed, upon heating the reaction mixture to 100 °C, the intensity of the signal at m/z = 257.2 decreased and a signal at m/z = 217.2 was detected, which is characteristic for tri-*n*-butylphosphine oxide $((n\text{-Bu})_3P{=}O)$. The formation of isobutene as well as $(n\text{-Bu})_3P{=}O$ in hydroamidation reactions was previously confirmed via GC- and NMR-spectroscopy.[29a]

We had previously dismissed mechanisms starting from Ru^0 intermediates (*Mechanisms A* and *D*), because we had never detected byproducts resulting from the reductive elimination of

7441

dx.doi.org/10.1021/ja111389r |*J. Am. Chem. Soc.* 2011, 133, 7428–7449

Figure 11. ESI—MS spectra for the *E*-selective hydroamidation of 2-pyrrolidinone (**1a**) and 1-hexyne (**5b**). (a) Heating to 100 °C for 5 min without 1-hexyne; (b) 40 min reaction time; (c) 150 min reaction time.

allyl fragments and had thus favored *Mechanism E*. However, this new experimental data gives at least indirect evidence for the formation of L_nRu^0 species, which unfortunately are particularly hard to detect by ESI—MS, because such species cannot be ionized by ligand dissociation.

We attempted to overcome this hurdle by using charged phosphine ligands. Unfortunately, the spectra obtained using [2-(dicyclohexylphosphino)ethyl] trimethylammonium chloride [$(C_6H_{11})_2P(C_2H_4)N(CH_3)_3Cl$] instead of $P(n\text{-Bu})_3$ were

inconclusive. Only few signals of ruthenium intermediates were detected, and they resulted mostly from ruthenium chloride species. In fact, we observed a strong signal at $m/z = 225.2$, which could unambiguously be assigned to a $[(cy)_2P(C_2H_4)]^+$ fragment (cy = cyclohexyl = C_6H_{11}), indicating that the trimethylamine entity is cleaved under the reaction conditions. The exchange of chloride by other counterions, for example, hexafluorophosphate, did not have any beneficial effect on the complexity of the resulting spectra. We also tried to induce a ligand
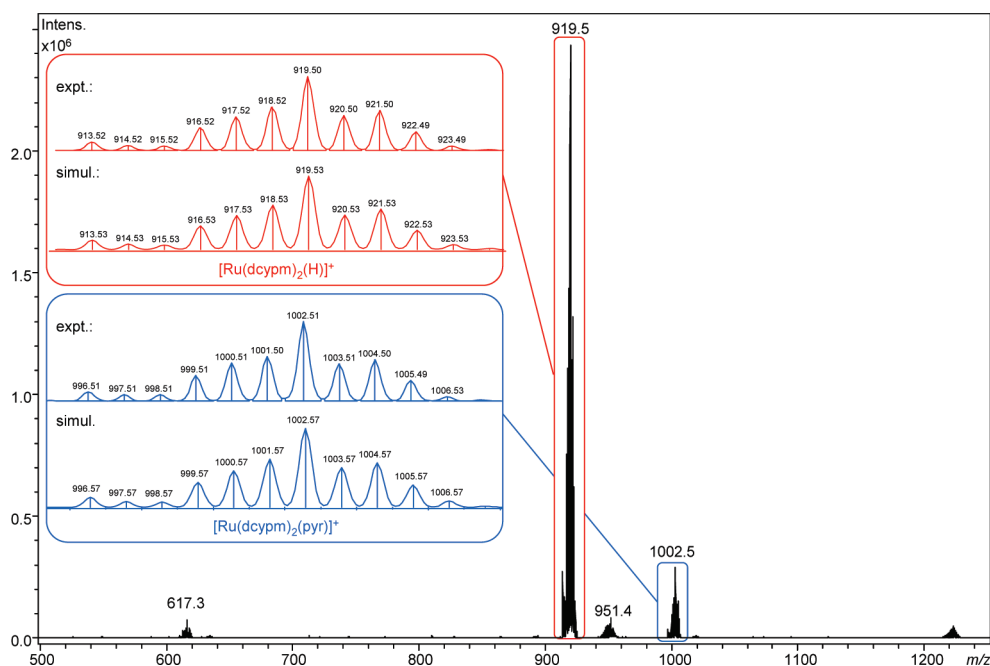
Figure 12. ESI−MS spectrum of a mixture of the catalyst and 2-pyrrolidinone (**1a**) under Z-selective hydroamidation conditions and after 5 min at 100 °C.

exchange of $P(n\text{-Bu})_3$ by $[(C_6H_{11})_2P(C_2H_4)N(CH_3)_3]^+$ in a preformed catalyst solution (2 mol % $(cod)Ru(met)_2$, 6 mol % $P(n\text{-Bu})_3$, 4 mol % DMAP) by adding the charged phosphine ligand afterward. Unfortunately, we could not observe any new Ru species in the corresponding ESI−MS spectra. The charged amonium phosphine ligand was simply not stable enough for in situ ESI−MS experiments. The syntheses of other non-amo-nium-based charged phosphine ligands, which are also suitable for hydroamidation reactions, are underway.

Next, we added 2-pyrrolidinone (**1a**) to the catalyst system consisting of 2 mol % of $(cod)Ru(met)_2$, 6 mol % of $P(n\text{-Bu})_3$ and 4 mol % of DMAP at 100 °C. At this stage, signals at $m/z = 712.3$ and 792.4 appeared, which, based on their location and exact isotope pattern, could be assigned to $[Ru(P(n\text{-Bu})_3)_2(DMAP)(pyr)]^+$ (pyr =2-pyrrolidinyl anion, $C_4H_6NO^-$) and $[Ru(P(n\text{-Bu})_3)_3$-$(pyr)]^+$ (Figure 11, Spectrum a).[26]

These species can result from the dissociation of a 2-pyrroli-dinyl anion $([M\text{-}(pyr)]^+)$ of $[Ru(P(n\text{-Bu})_3)_2(DMAP)(pyr)_2]$ and $[Ru(P(n\text{-Bu})_3)_3(pyr)_2]$ (Mechanisms B, C and E) but also from $[Ru(P(n\text{-Bu})_3)_2(DMAP)(pyr)(H)]$ and $[Ru(P(n\text{-Bu})_3)_3$-$(pyr)(H)]$ by protonation and H_2 release $([M + H]^+\text{-}H_2)$[49] during the ionization process (Mechanisms A and D).

1-Hexyne (**5b**) was then injected to the mixture and further samples were taken after 5, 15, 30, 40, 150, and 470 min at 100 °C (Figure 11, Spectra b and c, and Supporting Information).

Already after 5 min, the signals at $m/z = 712.3$ and 792.4 disappeared. Strong signals appeared at $m/z = 798.4$ and 833.5 and weaker signals at $m/z = 593.3, 675.4, 716.4, 757.5, 880.5,$ 921.7, 1003.8, and 1085.9.

The signals at $m/z = 833.5$ and 918.6 matched the calculated patterns for Ru−vinyl species $[Ru(P(n\text{-Bu})_3)_2(DMAP)_2(vinyl)]^+$ $(vinyl = C_6H_{11}^-)$ and $[Ru(P(n\text{-Bu})_3)_2(DMAP)_2(pyr)(vinyl)]$ $+ H^+$ (Figure 11, Spectrum b). They are both likely to result from the ionization of the $[Ru(P(n\text{-Bu})_3)_2(DMAP)_2(pyr)$-$(vinyl)]$ complex. Further fragmentation of this species via

ESI−MS−CID−MS (CID = collision-induced dissociation) was in agreement with the assignment and showed mainly the cleavage or the gradual decay of DMAP and $P(n\text{-Bu})_3$ ligands. This intermediate is in agreement with all postulated mechanisms.

The signal at $m/z = 716.4$ matched the calculated pattern for $[Ru(P(n\text{-Bu})_3)(DMAP)_2(pyr)(hex)(H)] + H^+$ (hex = C_6H_{10}) and the weak signal at $m/z = 631.3$ that of $[Ru(P(n\text{-Bu})_3)$-$(DMAP)_2(hex)(H)]^+$. Both species are likely to result from the ionization of a $[Ru(P(n\text{-Bu})_3)(DMAP)_2(pyr)(hex)(H)]$ com-plex. This might result from a Ru−vinyl complex such as **28** or **38** with a suitable ligand sphere $(m/z = 833.5)$, via vinyl/vinylidene rearrangement with concomitant dissociation of a $P(n\text{-Bu})_3$ ligand (consistent with Mechanisms C and D). The weak signals at $m/z = 751.5, 836.5,$ and 918.6 might be explained by $[Ru(P(n\text{-}Bu)_3)_2(DMAP)_2(H)]^+$, $[Ru(P(n\text{-Bu})_3)_2(DMAP)_2(pyr)(H)] +$ H^+ and $[Ru(P(n\text{-Bu})_3)_2(DMAP)_2(enamide)(H)] + H^+$ fragments (enamide = $C_{10}H_{16}NO^-$) resulting from the ioniza-tion of $[Ru(P(n\text{-Bu})_3)_2(DMAP)_2(pyr)(H)]$ (Mechanisms A and D) and $[Ru(P(n\text{-Bu})_3)_2(DMAP)_2(enamide)(H)]$ (Mechanisms A to E).

The species at $m/z = 798.4$ matched the pattern calculated for $[Ru(P(n\text{-Bu})_3)(DMAP)_2(enamide)(vinyl)] + H^+$ and might result from ionization of $[Ru(P(n\text{-Bu})_3)(DMAP)_2(enamide)$-$(vinyl)]$. The CID-fragmentation of this species showed the dissociation of a $P(n\text{-Bu})_3$ ligand and of a fragment with the mass of the enamide product (**6a**). As it contains two 1-hexyne (**5b**) molecules, this species is likely to be an intermediate in the formation of double alkyne insertion enamide products, which are observed as minor side products in hydroamidations. Its intensity decreases sharply after the first minutes of the reaction, while all other signals discussed above increased and the signal at $m/z = 833.5$ remained at a high level.

After the hydroamidation reaction was complete (150 min) the intensity of the signals pertaining to hydroamidation inter-mediates decreased, and a set of signals that had been detected at
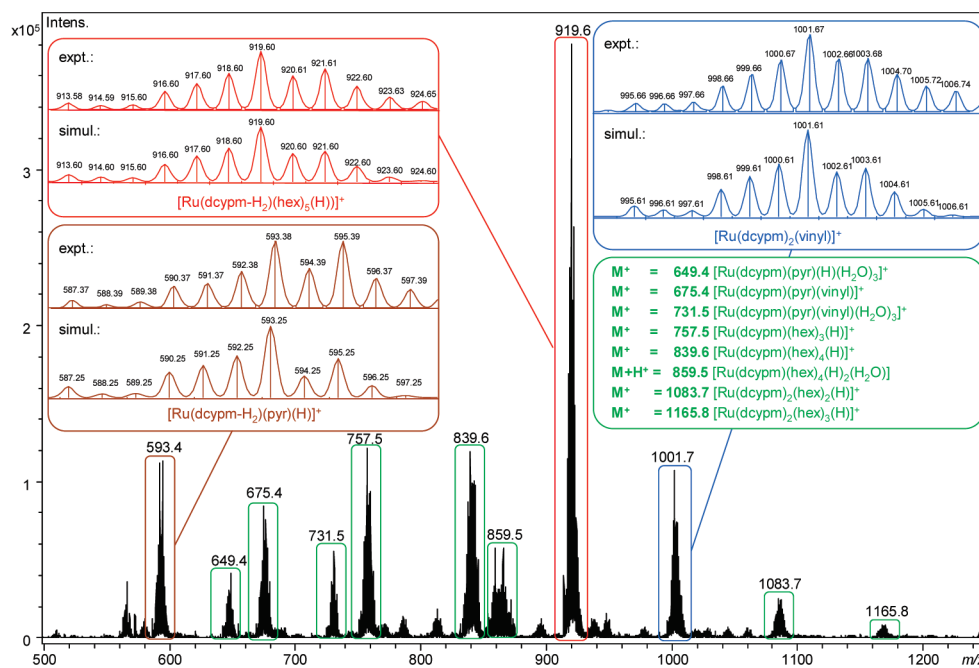
Figure 13. ESI−MS spectrum of a mixture of the catalyst, 2-pyrrolidinone (**1a**) and 1-hexyne (**5b**) under *Z*-selective hydroamidation conditions and after 5 min at 100 °C.

very low intensities earlier on, now became predominant. The signals at m/z = 593.4, 675.4, 757.4, 839.5, 921.6, 1003.7, and 1085.5 (Figure 11, Spectrum c) matched the calculated pattern for a series of Ru^{III} complexes with the chemical composition of $[Ru(P(n\text{-}Bu)_3)_2(pyr)(hex)_x(H)_2] + H^+$ bearing up to six 1-hexyne molecules (**5b**, $x = 0-6$). These species seem to be intermediates of alkyne oligomerization, which becomes the main reaction once most of the amide is consumed.

Next, we investigated the *Z*-selective hydroamidation of 2-pyrrolidinone (**1a**) and 1-hexyne (**5b**) in an analogous set of ESI−MS experiments.

A reaction mixture of the catalyst (2 mol % (cod)Ru(met)$_2$, 3 mol % dcypm, 8 equiv water) and 2-pyrrolidinone (**1a**) in toluene was heated to 100 °C for 5 min. The spectrum obtained at this stage showed two major signals at m/z = 919.5 and 1002.5, which, based on their location and exact isotope pattern, could be assigned to $[Ru(dcypm)_2(H)]^+$ (dcypm = bis-(dicyclohexylphosphino)methane, P$_2$C$_{25}$H$_{46}$) and $[Ru(dcypm)_2(pyr)]^+$ fragments (Figure 12).

Both cationic species seem to result from the same Ru-intermediate $[Ru(dcypm)_2(pyr)(H)]$. The formation of a Ru-intermediate such as **16** and **35** with a suitable ligand sphere can be explained best via oxidative addition of an amide to a neutral Ru^0-phosphine species (consistent with *Mechanisms A* and *D*). It is most likely that the cationic species are formed via dissociation of a 2-pyrrolidinyl anion ($[M\text{-}(pyr)]^+$) or protonation and H$_2$ release ($[M + H]^+$-H$_2$)[49] of $[Ru(dcypm)_2(pyr)(H)]$ during the ionization process. Further fragmentation of both species via ESI−MS−CID−MS (see Supporting Information) was in good agreement with this assignment and showed the same fragmentation species formed via gradual decay of dcypm and additionally via the cleavage of one 2-pyrrolidinyl anion from $[Ru(dcypm)_2(pyr)]^+$ in the case of the species at m/z = 1002.5.

We next injected 1-hexyne (**5b**) to the mixture and further samples were taken after 5, 25, 130, and 360 min at 100 °C (Figure 13 and Supporting Information).

After 5 min of heating in the presence of 1-hexyne (**5b**), the signals at m/z = 919.5 and 1002.5 disappeared and strong signals at m/z = 593.4, 757.5, 839.6, 919.6, and 1001.7 as well as weaker signals at m/z = 649.4, 675.4, 731.5, 859.5, 1083.7, and 1165.8 appeared. The masses often deviated by 2, 4, 6, or 8 mass units from expected molecular formulas. This can be explained with experiments by Leitner et al. who found that dcypb and bis-(dicyclohexylphosphino)propane (dcypp) ligands at Ru-centers easily dehydrogenate.[50] This thermal activation of sp^3 C−H bonds of bisphosphine Ru−bisallyl complexes leads to η^3-cyclooctenyl bridged Ru-complexes and extrusion of up to three protons from one cyclohexyl ring. We believe that similar dehydrogenation reactions took place under our hydroamidation reaction conditions. This would explain why signals that match $[M]^+ - 2, 4, 6,$ or 8 were detected.

The signal at m/z = 916.6 matched the calculated pattern of a $[Ru(dcypm\text{-}H_2)(hex)_5(H)]^+$ fragment (dcypm-H$_2$ = Cy$_2$P-(CH$_2$)P(Cy)(C$_6$H$_9$), formed via extrusion of H$_2$) and was confirmed to be nonidentical with the species at m/z = 915.5, observed in the absence of 1-hexyne (**5b**, Figure 12). The ESI−MS−CID−MS (see Supporting Information) of both signals were completely different. Whereas for the peak at m/z = 915.6, inter alia, the stepwise dissociation of four 1-hexyne (**5b**) molecules was observed, and for the peak at m/z = 915.5, stepwise decay of two phosphine ligands was observed. We believe that the species corresponding to the dominating signal at m/z = 915.6 is formed via dissociation of a 2-pyrrolidinyl anion ($[M\text{-}(pyr)]^+$) of $[Ru(dcypm\text{-}H_2)(hex)_5(pyr)(H)]$ or via protonation and H$_2$ release ($[M + H]^+$-H$_2$)[49] of $[Ru(dcypm)(hex)_5(H)_2]$, both presumably intermediates in alkyne oligomerization side reactions.

The smaller signal at m/z = 1001.7 could be assigned to a $[Ru(dcypm)_2(vinyl)]^+$ fragment likely to originate from a

Scheme 10. Catalytic Cycle for the *E*-Selective Hydroamidation of 1-Hexyne (**5b**) and 2-Pyrrolidinone (**1a**), L = ligand (P(*n*-Bu)₃ or DMAP)

[Ru(dcypm)₂(vinyl)(pyr)] species with the general formula **17**, **18** or **38**, formed by insertion of one 1-hexyne molecule (**5b**) into a Ru—H bond of **16** or **35** (consistent with *Mechanisms A and D*). The corresponding Ru—hydride—vinylidene species **39** would show the identical mass and isotope pattern. This is so, since both bidentate phosphine ligands would remain attached to the Ru center even if one of the Ru—P bonds is cleaved during the vinyl/vinylidene rearrangement step (consistent with *Mechanism D*).

Four Ru^{III} species could be assigned to the signals at m/z = 593.4, 649.4, 675.4, and 731.5 matching the calculated patterns of [Ru(dcypm-H₂)(pyr)(H)]$^+$, [Ru(dcypm)(pyr)(H)(H₂O)₃]$^+$, [Ru(dcypm)(pyr)(vinyl)]$^+$ and [Ru(dcypm)(pyr)(vinyl)-(H₂O)₃]$^+$ fragments. These species occur with only low intensities. They are most likely formed by oxidation side reaction during the sample extraction and injection into the ESI—MS instrument. Nevertheless, these Ru^{III} complexes—bearing 2-pyrrolidinyl-, hydrido-, and/or 1-hexenyl ligands—suggest that an oxidative addition step of the amide and an insertion step of the alkyne into a Ru—H bond is involved in the catalytic cycle of the *Z*-selective hydroamidation (consistent with *Mechanisms A and D*).

The five signals at m/z = 757.5, 839.6, 859.5, 1083.7, and 1165.8 match the calculated patterns of [Ru(dcypm)$_x$(hex)$_y$(H)]$^+$ species bearing one or two dcypm ligands (x = 1 or 2) and up to four 1-hexyne molecules (**5b**, y = 1—4). These species are also likely formed via dissociation of a 2-pyrrolidinyl anion ([M-(pyr)]$^+$) of [Ru(dcypm)$_x$(hex)$_y$(pyr)(H)] or via protonation and H₂ release ([M + H]$^+$-H₂)^{49} of [Ru(dcypm)$_x$(hex)$_y$(H)₂]. They constitute intermediates of the alkyne oligomerization side reaction.

After 25 min of heating, the intensities of all Ru-species remained at a high level and two new Ru-species at m/z = 865.5 and 947.6 could be detected (see Supporting Information). These new signals matched the calculated pattern of [Ru(dcypm)(hex)₃(OH)(tol)]$^+$ and [Ru(dcypm)(hex)₄(OH)(tol)]$^+$ fragments and are most likely formed via protonation and H₂ release ([M + H]$^+$-H₂)^{49} of [Ru-(dcypm)(hex)₃(H)(OH)(tol)].

The intensities of these two signals increased strongly in the spectra obtained after 130 and 360 min of heating, while the intensities of other signals decreased, indicating that the former correspond to oligomerization intermediates which predominate once most of the amide has been consumed.

■ CONCLUSIONS FROM THE EXPERIMENTAL STUDIES

Overall, most of the mechanisms under consideration were in disagreement with one or more experimental findings. *Mechanism A*, which involves an oxidative addition of the amide followed by an insertion of the alkyne into either the Ru—H or the Ru—N bond, correctly predicted the findings of the deuterium labeling experiments. It is also consistent with the detection of Ru—H species following addition of the amide to the Ru-catalyst and with most species detected by ESI—MS. However, it must be dismissed on the basis that a normal kinetic isotope effect was observed, while *Mechanism A* would have predicted an inverse
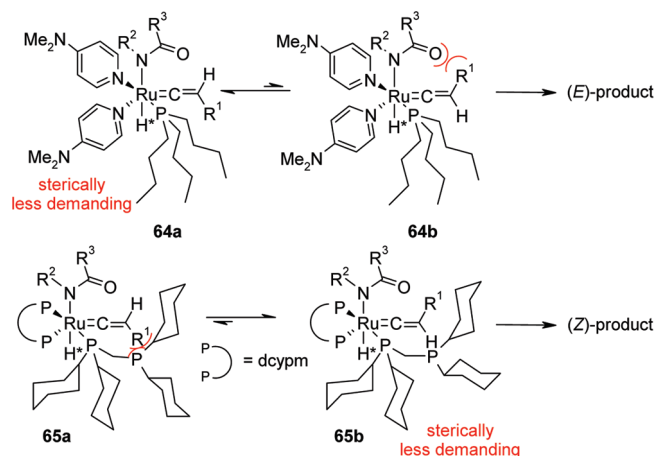
secondary kinetic isotope effect caused by a change in hybridization of the alkyne-C(1) carbon atom bond from sp to sp^2.

The same experimental findings also rule out the redox-neutral *Mechanism E*, which does not involve Ru—vinylidene intermediates, but instead proceeds via an attack of the amide nucleophile to a π-coordinated alkyne. This pathway is in good agreement with the isotope labeling and the ESI—MS studies, but offers no explanation for the observation of Ru—H-species after the addition of the amide to the catalyst system.

Mechanism B involves the formation of Ru—vinylidene species via 1,2-proton shift followed by an attack of the amide nucleophile. It must be excluded based on the results of the deuterium labeling studies, which unambiguously showed that in contrast to Ru-catalyzed additions of other nucleophiles, hydroamidations do not involve a shift of the terminal alkyne proton to the internal sp-carbon.

Mechanism C, which involves the formation of Ru—vinyl species and their rearrangement to Ru—hydride—vinylidene intermediates, is in agreement with most of the experimental findings. It correctly predicts the results of the deuterium labeling experiments and the observed normal kinetic isotope effect, and is in good agreement with most of the species observed in the ESI—MS studies. However, some of the cationic Ru^{IV} intermediates (**28**, **29** or **31**) should have been easily detectable by ESI—MS. One might also have expected the detection of Ru—H-species in the ^{1}H NMR in the presence of 1-hexyne (**5b**), rather than after the addition of 2-pyrrolidinone (**1a**) to the catalyst system. Moreover, it is unlikely that a protonation step with formation of cationic Ru—vinyl species is a favorable pathway in a nonpolar solvent under almost neutral conditions. The catalytic cycle involves only Ru-species in high oxidation states and offers no
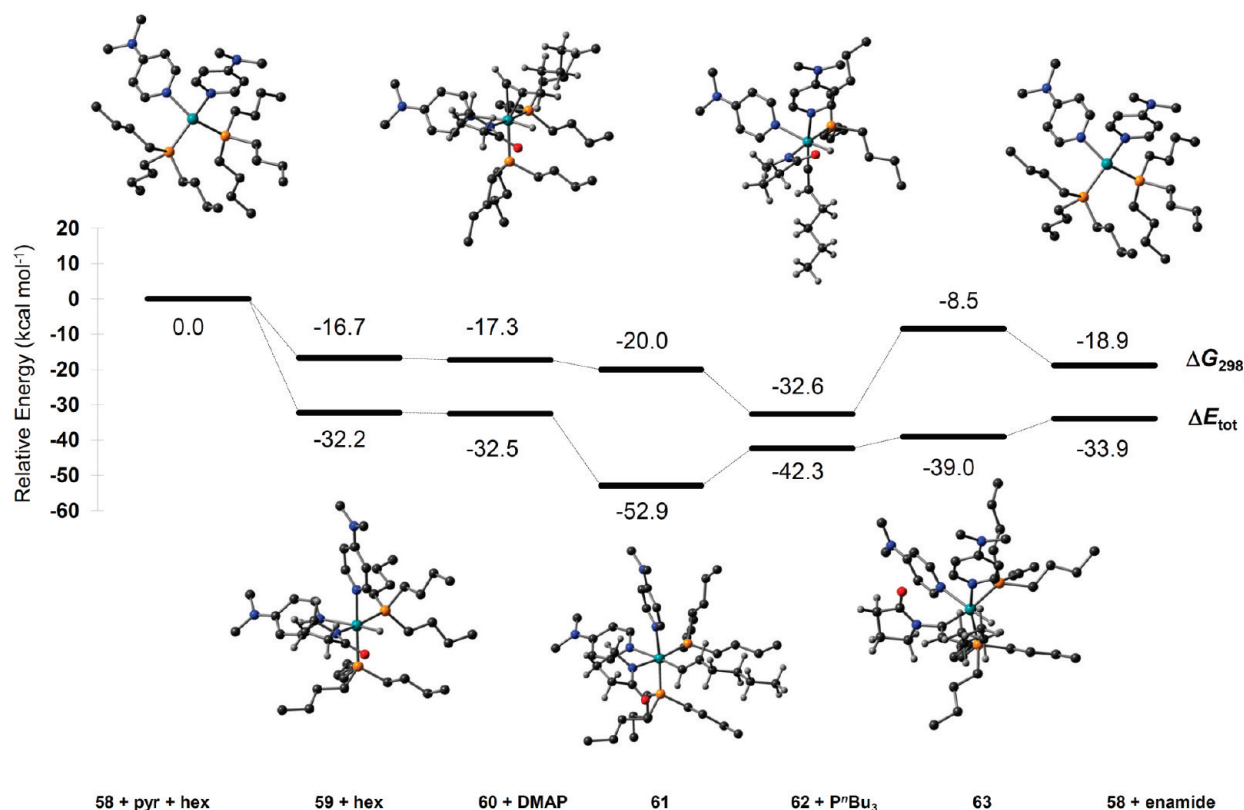
Scheme 11. Selectivity-Determining Step of the Hydroamidation Reaction

Figure 14. Relative energies and optimized structures of potential hydroamidation intermediates.

explanation for the detection of phosphonium salts known to arise from reductive deallylation processes.

Mechanism D is similar to *Mechanism C* in that it also involves Ru—vinyl intermediates that rearrange to Ru—hydride—vinylidene complexes. It is thus also in full agreement with the deuteration studies and correctly predicts the observed normal kinetic isotope effect. In contrast to *Mechanism C*, it starts from a Ru[0] species and thus offers a good explanation for the detection of phosphonium salts and of many Ru-species in the ESI—MS experiments. Moreover, the findings of the NMR studies are best explained by this mechanism, which starts with the oxidative addition of amides to the Ru-center with formation of Ru—H species. This would explain why after the addition of amides to the catalyst system, ^{1}H NMR signals below 0 ppm were detected, whereas these were not observed when only the alkyne was added to the catalyst.

For these combined reasons, the possible catalytic pathways can be narrowed down to a mechanism closely related to the proposed *Mechansim D*. On the basis of the experimental evidence, we believe that our model reaction, the *E*-selective hydroamidation of 1-hexyne (**5b**) with 2-pyrrolidinone (**1a**), proceeds via the mechanism depicted in Scheme 10.

The catalyst preformation proceeds via a reductive allylation process with release of a phosphorus ylide (**57**) and isobutene (**43**) and formation of a coordinatively unsaturated Ru[0] species bearing several neutral ligands. As the starting point for the depicted catalytic cycle we choose complex **58** with two phosphine and two DMAP ligands on the basis that intermediates with this combination of neutral ligands showed particularly strong signals in the in situ ESI—MS experiments. However, similar catalytic cycles with any combination of DMAP, phosphines, and solvent molecules would also be viable (MS signals at m/z = 751.5 $[M + H]^+$). Oxidative addition of the amide (**1a**) gives rise to an octahedral Ru—hydride complex **59**. This must be a slow step to be in accordance with the KIE of 2.3 found during the kinetic studies. The detection of signals at m/z = 751.5 and 836.5, which would match the $[M\text{-(pyr)}]^+$ and $[M + H]^+$ fragments of complex **59**, is in agreement with this pathway. In the next step, an alkyne (**5b**) coordinates to this species with dissociation of one neutral ligand (**60**). The alkyne then inserts into the Ru—H bond and the open coordination site created in the process is filled with a neutral ligand, leading to Ru[II]-vinyl intermediate **61**. Signals at m/z = 833.5 and 918.6 can be explained by the presence of $[M\text{-(pyr)}]^+$ and $[M + H]^+$ fragments of species **61**. The high intensity of the signal at m/z = 833.5 along with the observed KIE when using deuterated alkynes, indicates that this step is comparatively slow. 1,2-Hydride shift in Ru[II]—vinyl complex **61** then gives Ru[IV]—H—vinylidene species **62**. Only weak ESI—MS signals could be assigned to **62** (m/z = 631.3 $[M\text{-(pyr)}]^+$ and 716.4 $[M + H]^+$). Because of the δ^+ polarization at C(1) of the vinylidene moiety, **62** is susceptible to attack of the amide ligand to afford species **63**. A neutral ligand is likely to coordinate and to refill the empty coordination site. The signals detected at m/z = 751.5 ($[M\text{-(en-amide)}]^+$) and 918.6 ($[M + H]^+$) could be assigned to intermediate **63**. Finally, reductive elimination releases the enamide **6a**, regenerating the original catalytic species **58** and closing the catalytic cycle of the hydroamidation.

On the basis of the findings of the deuteration studies and the kinetic investigations, we assume that this pathway is also valid for related hydroamidations with other N—H nucleophiles. The studies presented above did not reveal any fundamental mechanistic differences between the *E*- and *Z*-selective protocols. On the basis of the NMR and ESI—MS studies with reaction mixtures of *Z*-selective hydroamidations, we believe that analogous species as those presented in Scheme 10 (**58**—**63**) are also present. The ligands are dcypm instead of P(*n*-Bu)$_3$ and DMAP before. However, in each step in which a vacant coordination site is required in the catalytic cycle (Scheme 10), one Ru—P bond of the bidentate ligand is cleaved, and therefore, the ligand remains coordinated to the Ru center leading to sterically more demanding Ru complexes. Hence, we conclude that the steric bulk of the ligand sphere is the decisive factor in directing the orientation of the substituent at the vinylidene moiety. As stretched in Scheme 11, the attack of the amide would then lead to enamides with different stereoselectivities depending on the preferred orientation of the vinylidene moiety relative to the amide. More in-depth studies are required to fully understand how the choice of ligands affects the stereoselectivity.

■ COMPUTATIONAL STUDIES

The Ru intermediates of the proposed catalytic cycle (Scheme 10, *Mechanism D*) have been identified based on ESI—MS and to some extent on NMR data. Since the information on the likely configuration of these intermediates is still limited, we used DFT calculations to look at the stability of each individual structure and possible spatial arrangements of the ligands. All calculations were performed using the Gaussian 03 or Gaussian 09 software package,[51] with B3LYP[52]/6-311+G(2d,p)[53]//B3LYP/6-31G-(d)[54] for H, C, N, O, P and Stuttgart RSC 1997 ECP[55] for Ru. A scaling factor for anharmonic corrections of vibrational frequencies of f = 0.9804 was used.[56]

A stable minimum was found for every postulated intermediate within the catalytic cycle. The calculated structures along with total energies and Gibbs free energies are depicted in Figure 14. The hydrogen atoms of the phosphine and DMAP ligands are omitted for clarity. Larger pictures of the optimized structures are included in the Supporting Information. The oxidative addition of 2-pyrrolidinone (**1a**) to the Ru species **58** with formation of the Ru—hydride complex **59** was calculated to be exothermic by $\Delta_r E_{tot}$ = −32.2 kcal mol^{-1} and exergonic by $\Delta_r G_{298}$ = −16.7 kcal mol^{-1}. The exchange reaction of DMAP by 1-hexyne (**5b**) to give a π-coordinated complex is almost thermoneutral ($\Delta_r E_{tot}$ = −0.3 kcal mol^{-1}, $\Delta_r G_{298}$ = −0.6 kcal mol^{-1}). The insertion of the alkyne in the Ru—H bond and refilling of the empty coordination site with one additional DMAP is exothermic and exergonic ($\Delta_r E_{tot}$ = −20.4 kcal mol^{-1}, $\Delta_r G_{298}$ = −2.7 kcal mol^{-1}). The following formation of vinylidene species **62** with the concomitant release of one phosphine ligand is endothermic ($\Delta_r E_{tot}$ = 10.6 kcal mol^{-1}) but exergonic ($\Delta_r G_{298}$ = −12.6 kcal mol^{-1}). The subsequent addition of the amide to the vinylidene moiety and the concomitant coordination of a neutral ligand is slightly endothermic ($\Delta_r E_{tot}$ = 3.3 kcal mol^{-1}) and highly endergonic ($\Delta_r G_{298}$ = 24.2 kcal mol^{-1}). The last reaction step, the reductive elimination of the enamide product requires only a small amount of total energy but releases a large amount of Gibbs free energy ($\Delta_r E_{tot}$ = 5.1 kcal mol^{-1}, $\Delta_r G_{298}$ = −10.4 kcal mol^{-1}). Overall, the computational studies support the conclusions drawn from the mechanistic studies. They confirm that the proposed catalytic cycle involves stable intermediates with comparable energies. Extensive computational studies using strongly simplified model systems are underway with the goal of calculating the transition states and obtaining reliably predicted kinetic isotope effects.

In summary, the results of our in-depth mechanistic studies of the hydroamidation support a catalytic cycle with ruthenium hydride and vinylidene species as the key intermediates. We thus propose that the reaction proceeds via an oxidative addition of the amide, followed by insertion of a π-coordinated alkyne into a ruthenium—hydride bond, rearrangement to a vinylidene species, nucleophilic attack of the amide, and finally reductive elimination of the product. This catalytic cycle is in agreement with all experimental results and is supported by DFT calculations that confirm the stability of all reaction intermediates.

■ ASSOCIATED CONTENT

ⓢ Supporting Information. Experimental procedures and full spectroscopic data of the deuterium-labeling, the in situ IR, the in situ NMR, the in situ ESI—MS and the competition experiments. This material is available free of charge via the Internet at http://pubs.acs.org.

■ AUTHOR INFORMATION

Corresponding Author
goossen@chemie.uni-kl.de; gns@chemie.uni-kl.de

■ ACKNOWLEDGMENT

■ REFERENCES

(1) Yet, L. *Chem. Rev.* **2003**, *103*, 4283–4306.

(2) Sugie, Y.; Dekker, K. A.; Hirai, H.; Ichiba, T.; Ishiguro, M.; Shiomi, Y.; Sugiura, A.; Brennan, L.; Duignan, J.; Huang, L. H.; Sutcliffe, J.; Kojima, Y. *J. Antibiot.* **2001**, *54*, 1060–1065.

(3) (a) McDonald, L. A.; Swersey, J. C.; Ireland, C. M.; Carroll, A. R.; Coll, J. C.; Bowden, B. F.; Fairchild, C. R.; Cornell, L. *Tetrahedron* **1995**, *51*, 5237–5244. (b) Boyd, M. R.; Farina, C.; Belfiore, P.; Gagliardi, S.; Kim, J. W.; Hahakawa, Y.; Beutler, J. A.; Mckee, T. C.; Bowman, B. J.; Bowman, E. J. *J. Pharmacol. Exp. Ther.* **2001**, *297*, 114–120.

(4) Davyt, D.; Entz, W.; Fernandez, R.; Mariezcurrena, R.; Mombrú, A. W.; Saldaña, J.; Domínguez, L.; Coll, J.; Manta, E. *J. Nat. Prod.* **1998**, *61*, 1560–1563.

(5) (a) Vidal, J.-P.; Escale, R.; Girard, J.-P.; Rossi, J.-C. *J. Org. Chem.* **1992**, *57*, 5857–5860. (b) Erickson, K. L.; Beutler, J. A.; Cardellina, J. H.; Boyd, M. R. *J. Org. Chem.* **1997**, *62*, 8188–8192. (c) Jansen, R.; Washausen, P.; Kunze, B.; Reichenbach, H.; Höfle, G. *Eur. J. Org. Chem.* **1999**, 1085–1089.

(6) Carbery, D. R. *Org. Biomol. Chem.* **2008**, *6*, 3455–3460.

(7) (a) Stevenson, P. J.; Graham, I. *ARKIVOC* **2003**, *7*, 139–144. (b) Gaulon, C.; Dhal, R.; Chapin, T.; Maisonneuve, V.; Dujardin, G. *J. Org. Chem.* **2004**, *69*, 4192–4202.

(8) Roff, G. J.; Lloyd, R. C.; Turner, N. J. *J. Am. Chem. Soc.* **2008**, *126*, 4098–4099.

(9) Willans, C. E.; Mulders, J. M. C. A.; de Vries, J. G.; de Vries, A. H. M. *J. Organomet. Chem.* **2003**, *687*, 494–497.

(10) Matsubara, R.; Nakamura, Y.; Kobayashi, S. *Angew. Chem.* **2004**, *116*, 1711–1713; *Angew. Chem. Int. Ed.* **2004**, *43*, 1679–1681.

(11) (a) van den Berg, M.; Minnaard, A. J.; Haak, R. M.; Leeman, M.; Schudde, E. P.; Meetsma, A.; Feringa, B. L.; de Vries, H. M.; Maljaars, E. P.; Wilians, C. E.; Hyett, D.; Boogers, A. F.; Hendricks, J. W.; de Vries, J. G. *Adv. Synth. Catal.* **2003**, *345*, 308–323. (b) Blaser, H.-U.; Malan, C.; Pugin, B.; Spindler, F.; Steiner, H.; Studer, M. *Adv. Synth. Catal.* **2003**, *345*, 103–151.

(12) (a) Dupau, P.; Le Gendre, P.; Bruneau, C.; Dixneuf, P. H. *Synlett* **1999**, 1832–1834. (b) Wang, X.; Porco, J. A., Jr. *J. Org. Chem.* **2001**, *66*, 8215–8221. (c) Bayer, A.; Maier, M. E. *Tetrahedron* **2004**, *60*, 6665–6677. (d) Adam, W.; Bosio, S. G.; Turro, N. J. *J. Org. Chem.* **2004**, *69*, 1704–1715. (e) Burk, M. J.; Casy, G.; Johnson, N. B. *J. Org. Chem.* **1998**, *63*, 6084–6098.

(13) (a) Brettle, R.; Mosedale, A. J. *J. Chem. Soc., Perkin Trans. 1* **1988**, 2185–2195. (b) Kuramochi, K.; Watanabe, H.; Kitahara, T. *Synlett* **2000**, 397–399. (c) Sato, M. *J. Org. Chem.* **1961**, *26*, 770–779.

(14) (a) Ager, D. J. *Synthesis* **1984**, 384–398. (b) Fürstner, A.; Brehm, C.; Cancho-Grande, Y. *Org. Lett.* **2001**, *3*, 3955–3957.

(15) Krompiec, S.; Pigulla, M.; Kuźnik, N.; Krompiec, M.; Marciniec, B.; Chadyniak, D.; Kasperczyk, J. *J. Mol. Catal. A: Chem.* **2005**, *225*, 91–101.

(16) (a) Wallace, D. J.; Klauber, D. J.; Chen, C.-Y.; Volante, R. P. *Org. Lett.* **2003**, *5*, 4749–4752; (b) Jiang, L.; Job, G. E.; Klapars, A.; Buchwald, S. L. *Org. Lett.* **2003**, *5*, 3667–3669; (c) Pan, X.; Cai, Q.; Ma, D. *Org. Lett.* **2004**, *6*, 1809–1812; (d) Brice, J. L.; Meerdink, J. E.; Stahl, S. S. *Org. Lett.* **2004**, *6*, 1845–1848; (e) Han, C.; Shen, R.; Su, S.; Porco, J. A., Jr. *Org. Lett.* **2004**, *6*, 27–30; (f) Tracey, M. R.; Hsung, R. P.; Antoline, J.; Kurtz, K. C. M.; Shen, L.; Slafer, B. W.; Zhang, Y. *Sci. Synth.* **2005**, *21*, 387–475; (g) Klapars, A.; Campos, K. R.; Chen, C.; Volante, R. P. *Org. Lett.* **2005**, *7*, 1185–1188; (h) Bolshan, Y.; Batey, R. A. *Angew. Chem.* **2008**, *120*, 2139–2142; *Angew. Chem. Int. Ed.* **2008**, *47*, 2109–2112.

(17) (a) Goossen, L. J.; Döhring, A. *Adv. Synth. Catal.* **2003**, *345*, 943–947. (b) Goossen, L. J.; Paetzold, J.; Winkel, L. *Synlett* **2002**, *10*, 1721–1723. (c) Goossen, L. J.; Ghosh, K. *Chem. Commun* **2001**, *20*, 2084–2085. (d) Goossen, L. J.; Goossen, K.; Rodríguez, N.; Blanchot, M.; Linder, C.; Zimmermann, B. *Pure Appl. Chem.* **2008**, *80*, 1725–1731.

(18) Heider, M.; Henkelmann, J.; Ruehl, T. EP 646571 **1995** [*Chem. Abstr.* **1995**, *123*, 229254].

(19) Kondo, T.; Tanaka, A.; Kotachi, S.; Watanabe, Y. *J. Chem. Soc. Chem. Commun* **1995**, 413–414.

(20) (a) Tokunaga, M.; Wakatsuki, Y. *Angew. Chem.* **1998**, *110*, 3024–3027; *Angew. Chem. Int. Ed.* **1998**, *37*, 2867–2869; (b) Tokunaga, M.; Suzuki, T.; Koga, N.; Fukushima, T.; Horiuchi, A.; Wakatsuki, Y. *J. Am. Chem. Soc.* **2001**, *123*, 11917–11924; (c) Grotjahn, D. B.; Incarvito, C. D.; Rheingold, A. L. *Angew. Chem.* **2001**, *113*, 4002–4005; *Angew. Chem. Int. Ed.* **2001**, *40*, 3884–3887; (d) Chevallier, F.; Breit, B. *Angew. Chem.* **2006**, *118*, 1629–1632; *Angew. Chem. Int. Ed.* **2006**, *45*, 1599–1602. (e) Labonne, A.; Kribber, T.; Hintermann, L. *Org. Lett.* **2006**, *8*, 5853–5856. (f) Hintermann, L.; Kribber, T.; Labonne, A.; Paciok, E. *Synlett* **2009**, 2412–2416.

(21) (a) Rotem, M.; Shvo, Y. *Organometallics* **1983**, *2*, 1689–1691. (b) Mitsudo, T.; Hori, Y.; Yamakawa, Y.; Watanabe, Y. *J. Org. Chem.* **1987**, *52*, 2230–2239. (c) Ruppin, C.; Dixneuf, P. H. *Tetrahedron Lett.* **1986**, *27*, 6323–6324. (d) Philippot, K.; Devanne, D.; Dixneuf, P. H. *J. Chem. Soc. Chem. Commun* **1990**, 1199–1200. (e) Neveux, M.; Seiller, B.; Hagedorn, F.; Bruneau, C.; Dixneuf, P. H. *J. Organomet. Chem.* **1993**, *451*, 133–138. (f) Goossen, L. J.; Paetzold, J.; Koley, D. *Chem. Commun* **2003**, 706–707.

(22) (a) Uchimaru, Y. *Chem. Commun* **1999**, 1133–1134; (b) Tokunaga, M.; Eckert, M.; Wakatsuki, Y. *Angew. Chem.* **1999**, *111*, 3416–3419; *Angew. Chem. Int. Ed.* **1999**, *38*, 3222–3225. (c) Kondo, T.; Okada, T.; Suzuki, T.; Mitsudo, T.-a. *J. Organomet. Chem.* **2001**, *622*, 149–154. (d) Fukumoto, Y.; Dohi, T.; Masaoka, H.; Chatani, N.; Murai, S. *Organometallics* **2002**, *21*, 3845–3847. (e) Shimada, T.; Yamamoto, Y. *J. Am. Chem. Soc.* **2003**, *125*, 6646–6647. (f) Yi, C. S.; Yun, S. Y.; Guzei, I. A. *J. Am. Chem. Soc.* **2005**, *127*, 5782–5783. (g) Li, Y.; Marks, T. J. *Organometallics* **1996**, *15*, 3770–3772. (h) Li, Y.; Marks, T. J. *J. Am. Chem. Soc.* **1998**, *120*, 1757–1771.

7448

dx.doi.org/10.1021/ja111389r |*J. Am. Chem. Soc.* 2011, 133, 7428–7449

(23) Koelle, U.; Rietmann, C.; Tjoe, J.; Wagner, T.; Englert, U. *Organometallics* **1995**, *14*, 703–704.

(24) (a) Gemel, C.; Trimmel, G.; Slugovc, C.; Kremel, S.; Mereiter, K.; Schmid, R.; Kirchner, K. *Organometallics* **1996**, *15*, 3998–4004. (b) Varela-Fernández, A.; González-Rodríguez, C.; Varela, J. A.; Castedo, L.; Saá, C. *Org. Lett.* **2009**, *11*, 5350–5353. (c) Liu, P. N.; Su, F. H.; Wen, T. B.; Sung, H. H.-Y. *Chem.—Eur. J.* **2010**, *16*, 7889–7897.

(25) Goossen, L. J.; Rauhaus, J. E.; Deng, G. *Angew. Chem.* **2005**, *117*, 4110–4113; *Angew. Chem. Int. Ed.* **2005**, *44*, 4042–4045.

(26) Goossen, L. J.; Arndt, M.; Blanchot, M.; Rudolphi, F.; Menges, F.; Niedner-Schatteburg, G. *Adv. Synth. Catal.* **2008**, *350*, 2701–2707.

(27) Goossen, L. J.; Blanchot, M.; Salih, K. S. M.; Karch, R.; Rivas-Nass, A. *Org. Lett.* **2008**, *10*, 4497–4499.

(28) Goossen, L. J.; Blanchot, M.; Brinkmann, C.; Goossen, K.; Karch, R.; Rivas-Nass, A. *J. Org. Chem.* **2006**, *71*, 9506–9509.

(29) (a) Goossen, L. J.; Salih, K. S. M.; Blanchot, M. *Angew. Chem.* **2008**, *120*, 8620–8623; *Angew. Chem. Int. Ed.* **2008**, *47*, 8492–8495. (b) Goossen, L. J.; Blanchot, M.; Salih, K. S. M.; Goossen, K. *Synthesis* **2009**, 2283–2282.

(30) Buba, A. E.; Arndt, M.; Goossen, L. J. *J. Organomet. Chem.* **2010**, *696*, 170–178.

(31) Goossen, L. J.; Blanchot, M.; Arndt, M.; Salih, K. S. M. *Synlett* **2010**, 1685–1687.

(32) (a) Bruneau, C.; Dixneuf, P. H. *Angew. Chem.* **2006**, *118*, 2232–2260; *Angew. Chem. Int. Ed.* **2006**, *45*, 2176–2203. (b) Rigaut, S.; Touchard, D.; Dixneuf, P. H. *Coord. Chem. Rev.* **2004**, *248*, 1585–1601.

(33) Oliván, M.; Clot, E.; Eisenstein, O.; Caulton, K. G. *Organometallics* **1998**, *17*, 3091–3100.

(34) DFT calculations confirmed that the reaction of 2-pyrrolidinone (**1a**) and deprotonated *N*-((*E*)-hex-1-enyl)pyrrolidin-2-one, leading to the 2-pyrrolidinyl anion and the corresponding enamide (**6a**), is both exotherm ($\Delta_r E_{tot} = -30.88$ kcal mol^{-1}) and exergonic ($\Delta_r G_{298} = -30.02$ kcal mol^{-1}).

(35) Although there is no experimental proof in literature that the rehybridisation from sp to sp^2 causes an inverse isotope effect, it must be expected based on the analogy to sp^2/sp^3 rehybridizations. See for example: Carey, F. A.; Sundberg, R. J. *Advanced Organic Chemistry*, Third edition; Plenum Press: New York, London, 1990; pp 216–218. The same assumption was made, e.g., in: Ipaktschi, J.; Mohsseni-Ala, J.; Uhlig, S. *Eur. J. Inorg. Chem.* **2003**, 4313–4320.

(36) Maegawa, T.; Fujiwara, Y.; Inagaki, Y.; Monguchi, Y.; Sajiki, H. *Adv. Synth. Catal.* **2008**, *350*, 2215–2218.

(37) Rigaut, S.; Perruchon, J.; Guesmi, S.; Fave, C.; Touchard, D.; Dixneuf, P. H. *Eur. J. Inorg. Chem.* **2005**, 447–460.

(38) Ryabov, A. D. *Chem. Rev.* **1990**, *90*, 403–424.

(39) Ciardi, C.; Reginato, G.; Gonsalvi, L.; de los Rios, I.; Romerosa, A.; Peruzzini, M. *Organometallics* **2004**, *23*, 2020–2026.

(40) Choe, J.-I.; Choi, H.-S.; Kuczkowski, R. L. *Magn. Reson. Chem.* **1986**, *24*, 1044–1047.

(41) Touchard, D.; Haquette, P.; Pirio, N.; Toupet, L.; Dixneuf, P. H. *Organometallics* **1993**, *12*, 3132–3139.

(42) (a) Bruneau, C.; Dixneuf, P. H. *Acc. Chem. Res.* **1999**, *32*, 311–323. (b) Vijayaraj, T. A.; Sundararajan, G. *J. Mol. Catal. A* **1995**, *99*, 47–54.

(43) Caballero, A.; Jalón, F. A.; Manzano, B. R. *Chem. Commun* **1998**, 1879–1880.

(44) (a) Guerchais, V.; Lapinte, C.; Thepot, J. Y.; Toupet, L. *Organometallics* **1988**, *7*, 604–612. (b) Maurer, J.; Linseis, M.; Sarkar, B.; Schwederski, B.; Niemeyer, M.; Kaim, W.; Zli, S.; Anson, C.; Zabel, M.; Winter, R. F. *J. Am. Chem. Soc.* **2008**, *130*, 259–268. (c) Jung, S.; Ilg, K.; Brandt, C. D.; Wolf, J.; Werner, H. *Eur. J. Inorg. Chem.* **2004**, 469–480. (d) Bassetti, M.; Cadierno, V.; Gimeno, J.; Pasquini, C. *Organometallics* **2008**, *27*, 5009–5016.

(45) Cabeza, J. A.; Riera, V. *J. Organomet. Chem.* **1989**, *376*, C23–C25.

(46) (a) Hinderling, C.; Adlhart, C.; Chen, P. *Angew. Chem.* **1998**, *110*, 2831–2835; *Angew. Chem. Int. Ed.* **1998**, *37*, 2685–2689. (b) Adlhart, C.; Hinderling, C.; Baumann, H.; Chen, P. *J. Am. Chem. Soc.*

2000, *122*, 8204–8214. (c) Frech, C. M.; Blacque, O.; Schmalle, H. W.; Berke, H.; Adlhart, C.; Chen, P. *Chem.—Eur. J.* **2006**, *12*, 3325–3338.

(47) (a) Markert, C.; Pfaltz, A. *Angew. Chem.* **2004**, *116*, 2551–2554; *Angew. Chem. Int. Ed.* **2004**, *43*, 2498–2500; (b) Markert, C.; Neuburger, M.; Kulicke, K.; Meuwly, M.; Pfaltz, A. *Angew. Chem.* **2007**, *119*, 5996–5999; *Angew. Chem. Int. Ed.* **2007**, *46*, 5892–5895; (c) Markert, C.; Rosel, P.; Pfaltz, A. *J. Am. Chem. Soc.* **2008**, *130*, 3234–3235; (d) Teichert, A.; Pfaltz, A. *Angew. Chem.* **2008**, *120*, 3408–3410; *Angew. Chem. Int. Ed.* **2008**, *47*, 3360–3362. (e) di Lena, F.; Matyjaszewski, K. *Chem. Commun.* **2008**, 6306–6308. (f) di Lena, F.; Matyjaszewski, K. *Dalton Trans.* **2009**, 8884–8890.

(48) Kuran, W.; Musco, A. *Inorg. Chim. Act.* **1975**, *12*, 187–193.

(49) Reinhardt, B. M.; Niedner-Schatteburg, G. *J. Phys. Chem. A* **2002**, *106*, 7988–7992.

(50) Six, C.; Gabor, B.; Görls, H.; Mynott, R.; Philipps, P.; Leitner, W. *Organometallics* **1999**, *18*, 3316–3326.

(51) (a) Gaussian 03, Revision E.01, Gaussian, Inc.: Wallingford CT, 2004. (b) Gaussian 09, Revision A.02, Gaussian, Inc.: Wallingford CT, 2009; for full citations see the Supporting Information.

(52) (a) Lee, C.; Yang, W.; Parr, R. G. *Phys. Rev. B* **1988**, *37*, 785–789. (b) Becke, A. D. *J. Chem. Phys.* **1993**, *98*, 5648–5652. (c) Stephens, P. J.; Devlin, J. F.; Chabalowski, C. F.; Frisch, M. J. *J. Phys. Chem.* **1994**, *98*, 11623–11627.

(53) Krishnan, R.; Binkley, J. S.; Seeger, R.; Pople, J. A. *J. Chem. Phys.* **1980**, *72*, 650–654.

(54) Hariharan, P. C.; Pople, J. A. *Theor. Chim. Acta* **1973**, *28*, 213–222.

(55) Andrae, D.; Häussermann, U.; Dolg, M.; Stoll, H.; Preuss, H. *Theor. Chim. Acta* **1990**, *77*, 123–141.

(56) Wong, M. W. *Chem. Phys. Lett.* **1996**, *256*, 391–399.

7449

dx.doi.org/10.1021/ja111389r |*J. Am. Chem. Soc.* 2011, 133, 7428–7449